# SANDIA REPORT

SAND2001-0310
Unlimited Release
Printed February 2001

# Phase Partitioning of TNT and DNT in Soils

J. M. Phelan and J. L. Barnett

Prepared by
Sandia National Laboratories
Albuquerque, New Mexico 87185 and Livermore, California 94550

Sandia is a multiprogram laboratory operated by Sandia Corporation, a Lockheed Martin Company, for the United States Department of Energy under Contract DE-AC04-94AL85000.



Issued by Sandia National Laboratories, operated for the United States Department of Energy by Sandia Corporation.



Available to DOE and DOE contractors from
U.S. Department of Energy
Office of Scientific and Technical Information
P.O. Box 62
Oak Ridge, TN 37831

Telephone: (865)576-8401
Facsimile: (865)576-5728
E-Mail: reports@adonis.osti.gov
Online ordering: http://www.doe.gov/bridge

Available to the public from
U.S. Department of Commerce
National Technical Information Service
5285 Port Royal Rd
Springfield, VA 22161

Telephone: (800)553-6847
Facsimile: (703)605-6900
E-Mail: orders@ntis.fedworld.gov
Online order: http://www.ntis.gov/ordering.htm

SAND2001-0310
Unlimited Release
Printed February 2001

# Phase Partitioning of TNT and DNT in Soils

J.M. Phelan
Environmental Restoration Technologies Department

J.L. Barnett
Explosive Materials and Subsystems Department

Sandia National Laboratories
P.O. Box 5800
Albuquerque, NM 87185-0719

## Abstract

Detecting the presence of a buried landmine or unexploded ordnance using explosive chemical vapors has been considered possible with advances in sensitivity and selectivity of emerging chemical sensing technologies. Sampling and analysis of explosive vapors emanating from soils is a significant challenge due to the low vapor concentrations produced through this process. Understanding the environmental impacts to this chemical signature is also important, as environmental factors have a dramatic effect on the transfer of the chemical mass between soil solid, liquid and vapor phases. This work was completed to assess the phase partitioning phenomena of two explosive chemical materials (2,4,6-TNT and 2,4-DNT) typically found in landmines and ordnance. Laboratory measurements of water solubility, soil-water partitioning, and soil-vapor partitioning were completed in the absence of literature values. An integrated soil system partitioning analysis was completed using soil physics phase partitioning theory for use in evaluation of the impact of environmental factors. Using estimates of soil residues from samples adjacent to buried landmines and ordnance, performance requirements for vapor sensing buried landmines and unexploded ordnance have been estimated.

## Acknowledgements

This work was sponsored by the Defense Advanced Research Projects Agency, Dog's Nose Program, under the direction of Dr. Regina Dugan and Ms. Vivian George for application to landmines and by the Strategic Environmental Research and Development Program, under the direction of Dr. Jeff Marqusee for application to unexploded ordnance. Sandia is a multiprogram laboratory operated by Sandia Corporation, a Lockheed Martin Company, for the United States Department of Energy under Contract DE-AC04-94AL85000.

# Contents



# List of Figures

## List of Tables

# 1.0 Introduction

The majority of explosives found in antipersonnel and antitank landmines contain 2,4,6-trinitrotoluene (TNT). 2,4-Dinitrotoluene (DNT) is a common manufacturing byproduct in the synthesis of TNT (Kaye, 1980; Urbanski, 1964) and is believed to be a principal component suitable for detection of buried landmines (George et al., 2000). Recent efforts to develop an electronic dog's nose have prompted a careful evaluation of the transport of chemical signatures from buried landmines through the soil to the ground surface. One goal of this effort is to understand the performance envelope that chemical sensors need to perform within in order to be successful.

The soil environment is complex with interactions between soil particles, soil air, and soil water. This is compounded with partitioning of organic chemicals such as TNT and DNT sorbed onto soil particles, as a vapor in soil air, and as a solute in soil water. Figure 1 shows the principal phase partitioning processes that TNT and DNT participate in when present in surface soils.

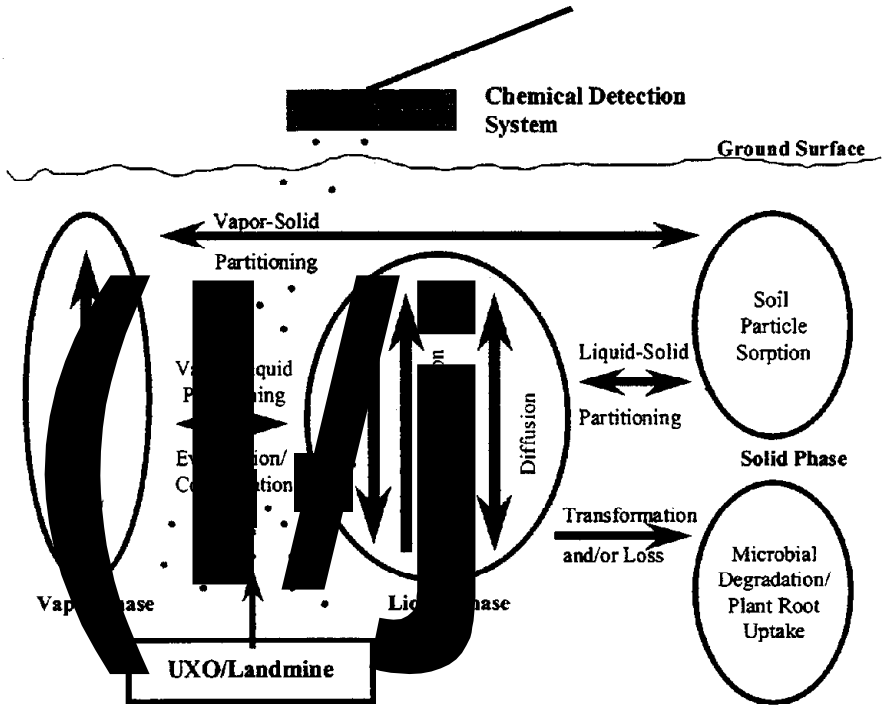


Figure 1. Phase Partitioning Components in a Soil System

This report documents the soil phase partitioning phenomena of TNT and DNT in soils. Where existing data were not available, measurements were performed on a single soil using both standard and novel methods. The phase partitioning interactions have been compiled into a spreadsheet to evaluate the impacts to phase transfers and estimate the magnitude of phase specific concentrations with variations in property inputs. With this knowledge, estimates of vapor phase chemical sensing performance requirements can be developed for various environmental conditions (e.g. soil type and soil wetness).

# 2.0 Water Solubility

## 2.1 Background

Water solubility of TNT has been reported by many reference handbooks (Stephen and Stephen, 1963; Verschueren, 1983; Urbansky, 1964) based on the work of Taylor and Rinkenbach, 1923. A recent study and review (Ro et al., 1996) has shown that the data of Taylor and Rinkenbach, 1923 may be biased high by about 50%. Solubility data for DNT are very limited with most reports (McGrath, 1995; Rosenblatt, 1991; Urbanski, 1964) referring to a summary in Army Materiel Command, 1971 showing values of (0.027, 0.037 and 0.254) g/ 100g at (22, 50 and 100 °C), respectively. In this work, additional water solubility measurements were completed for TNT and DNT in the temperature range expected in near surface soils. The details of this work are repeated here for completeness and are also published in Phelan and Barnett, 2001.

## 2.2 Materials and Methods

The aqueous solubility of DNT and TNT was measured by direct sampling of a suspension of crystalline material in deionized water. Filtration of the samples was not performed due to concerns with loss of analyte on filter media. A 125 mL Erlenmeyer flask was filled with 100 mL of deionized water and placed into a constant temperature bath. The water was stirred using a teflon-coated magnetic stirring bar. The water temperature was controlled by a constant-temperature water bath (Neslab, Model RTE-101) recirculated through a copper coil in the water bath. Approximately 100 mg of 2,4-Dinitrotoluene (Aldrich) was placed into the water and allowed to mix for 1 week. Military grade TNT (recrystalized three times) was used with about the same starting conditions as the DNT.

All volumetric measures were first determined gravimetrically (+/- 0.00001 g ) then converted to volumetric values with density values at 22.8 °C. Water samples (~1 mL) were collected by disposable pipette and placed into a 10 mL vial containing about 6 mL of deionized water to limit precipitation, especially from the higher temperature conditions. To determine if any chemical residue remained in the pipette, about 1.5 mL of acetonitrile ($CH_3CN$) was imbibed then placed into a 2 mL autosampler vial for quantitation. Three water and three acetonitrile wash samples were obtained at each temperature. The temperature was started at the low end and ramped up to the top end, then returned back to the low end. Temperature was measured with a mercury thermometer (+/- 0.1 °C) The solution remained at the desired temperature for 2 to 7 days before samples were taken. Each DNT sample was analyzed in duplicate and each TNT sample was analyzed in triplicate.

The water samples were analyzed by RP-HPLC using a Waters 600E System Controller, Waters 717 plus Autosampler, and Waters 996 Photodiode Array. Samples were injected (10 µl) into Brownlee Spheri-5 RP-18 5 µm 4.6x250 mm column and eluted with a 65:35 methanol+water run in isocratic mode. The photodiode array was run in scan mode accumulating all peaks found from 230 to 400 nm for the elution time of DNT or TNT.

The acetonitrile wash sample was quantified with a 1 µL injection into an HP 6890 Gas Chromatograph equipped with a micro electron capture detector and a 0.53mm x 6 m RTX 225 0.1 µm film thickness column. The split/splitless injector was programmed for a 220 °C inlet temperature, starting column temperature of 100 °C for 2 min, ramped to 200 °C at 10 °C/min, then held for 7 min.

## 2.3 Results and Discussion.

Tables 1 and 2 summarize the solubility data for DNT and TNT, respectively. While the total (sum of water sample and acetonitrile wash) appears to be larger for each temperature, there is no statistically significant difference ($p<0.05$).

Table 1. Solubility of 2,4-DNT (mg/L)

| Temp(°C) | Water plus $CH_3CN$ Rinse | | Water Sample Only | | |
|---|---|---|---|---|---|
| | Mean | S.D. | Mean | S.D. | Approach |
| 12.4 | 130 | 3.0 | 129 | 2.9 | Rising |
| 22.0 | 189 | 6.1 | 188 | 5.3 | Rising |
| 21.7 | 183 | 4.8 | 182 | 4.2 | Rising |
| 32.0 | 270 | 1.3 | 269 | 1.1 | Rising |
| 42.0 | 418 | 1.3 | 416 | 1.2 | Rising |
| 51.0 | 610 | 1.9 | 608 | 1.8 | Rising |
| 61.8 | 983 | 5.7 | 975 | 8.5 | Rising |
| 41.2 | 400 | 1.7 | 397 | 0.8 | Falling |
| 25.2 | 200 | 2.3 | 199 | 2.2 | Falling |

Table 2. Solubility of 2,4,6-TNT (mg/L)

| Temp (°C) | Water plus $CH_3CN$ Rinse | | Water Sample Only | | |
|---|---|---|---|---|---|
| | Mean | S.D. | Mean | S.D. | Approach |
| 13.9 | 91 | 7.9 | 86 | 1.8 | Rising |
| 23.0 | 116 | 2.4 | 115 | 2.1 | Rising |
| 33.3 | 191 | 0.7 | 191 | 0.5 | Rising |
| 42.6 | 266 | 0.6 | 266 | 0.7 | Rising |
| 51.8 | 428 | 3.7 | 427 | 3.4 | Rising |
| 61.0 | 643 | 3.4 | 641 | 4.6 | Rising |
| 33.2 | 192 | 8.0 | 191 | 6.8 | Falling |
| 13.6 | 90 | 1.3 | 90 | 1.3 | Falling |
| 13.6 | 92 | 1.0 | 92 | 1.0 | Falling |

Figure 2 shows the total solubility values for DNT as compared to the Army Materiel Command (1971) data. Data from this study show very different results from the Army data with values 30% less at 22 °C and 65% greater at 50 °C. Figure 3 compares the TNT results from this study to that of Ro et al. (1996), Spanggord et al. (1983), and Taylor and Rinkenbach (1923). Results from this work show TNT values consistently less than Taylor and Rinkenbach (1923) but greater than that of Ro et al. (1996). The data are very consistent with data reported by Spanggord (1983). For both DNT and TNT, visible precipitation occurred in the sampling pipette in the short time during transfer to the vial for only the >60 °C condition. Solubility data for DNT reported here were very different from previously reported values. However, the values were repeatable when comparing rising to temperature and falling to temperature conditions. The TNT data were consistent with past reported data, bridging a gap between two data sets and very close to one other.

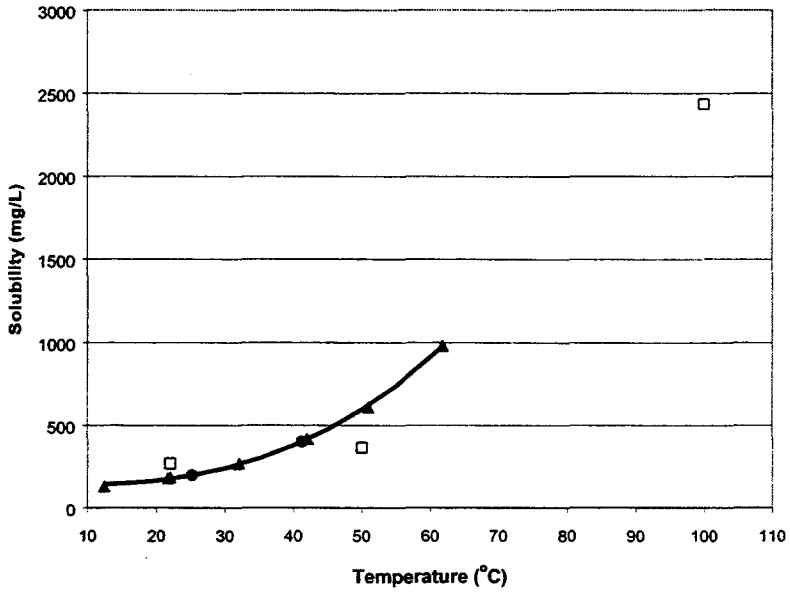


Figure 2. DNT Solubility: (□)Army Materiel Command (1971); (▲)This study, rising to temperature; (●) This study, falling to temperature; (——) This study curve fit (Table 3).

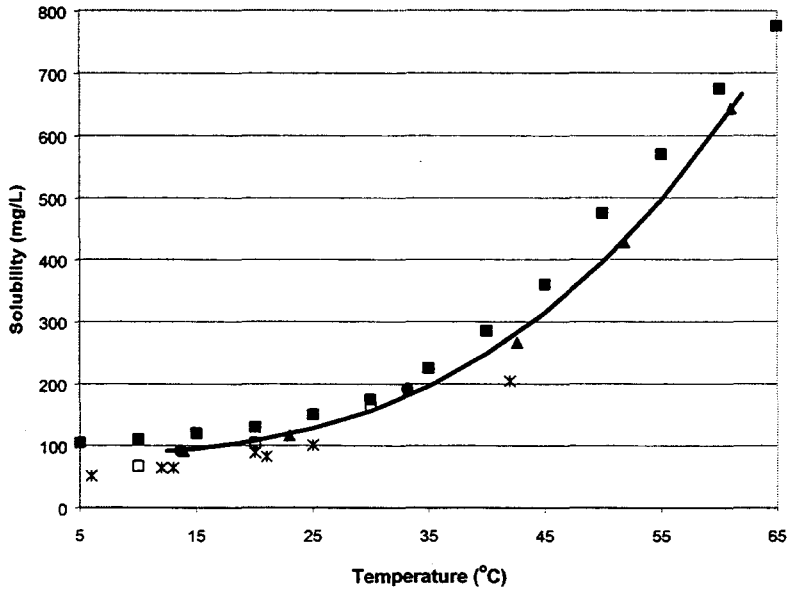


Figure 3. TNT solubility: (■)Taylor and Rinkenbach (1923), interpolated data; (▲)This study, rising to temperature (●); This study, falling to temperature; (*) Ro et al., 1996; (□) Spanggord, 1983; (-----) This study curve fit (Table 3).

An empirical relationship of water solubility is needed in the evaluation of temperature sensitive phase partitioning phenomena (see Section 5). A simple power function was determined by curve fitting (Table Curve 2D, Ver. 4, SPSS Inc.) with the results shown in Table 3.

Table 3. Aqueous Solubility Empirical Correlation [$y = a+b(T/°C)^c$]

| | a | b | c |
|---|---|---|---|
| DNT | 135.59 | 0.0064382 | 2.8569 |
| TNT | 86.045 | 0.0034874 | 2.9131 |

# 3.0 Soil-Water Partitioning

## 3.1 Background

Movement of explosive chemical signatures emitted from shallow buried UXO and landmines are strongly dependent on the soil-water partitioning coefficient (Phelan and Webb, 1997). Little data exist on the soil-water partitioning coefficient for DNT. One estimate of the log $K_{oc}$ for DNT indicates a value of 2.4 from the Cornhusker Army Ammunition Plant (Rosenblatt, 1986). In this work, batch adsorption studies were performed for DNT on a single soil used in various chemical transport experiments from Sandia National Laboratories, Albuquerque, NM following the methods of Pennington and Patrick, 1990.

## 3.2 Materials and Methods

Surface soil was obtained down to a depth of 15 to 20 cm in an area due west of the Sandia National Laboratories Landmine Test Facility. Soils were sieved through a 2 mm screen, mixed and air-dried. These soils have been found to be uncontaminated with explosive constituents. Properties of this soil are shown in Table 4.

Table 4. Soil Properties used in Batch Adsorption Experiments

| Property | Value |
|---|---|
| Sand | 71 % |
| Silt | 21 % |
| Clay | 8 % |
| Fraction Organic Carbon - $f_{OC}$ | 0.8 % |
| Cation Exchange Capacity - CEC | 32 meq/100g |

Stock DNT solutions were prepared by dissolving pure crystalline compound (Aldrich) in deionized water containing 0.005 M $Ca(NO_3)_2$. Dilutions were prepared to make concentrations of 0.5, 0.75, 1.0, 1.25, 1.5 and 2.0 mg/L. A second set of solutions at higher concentrations were prepared at 25, 50, 75, 100, 125 and 150 mg/L. Soils (4 g) were equilibrated with 16 mL of solution for about 18 hours on a rotating tumbler. Kinetic adsorption studies were not performed, however, data on TNT showed similar batch equilibration tests reached steady state within 2-4 hours, with low concentrations (< 4 mg/L) reaching apparent equilibrium (Pennington and Patrick, 1990). The entire solution was placed in a centrifuge and run at 3500 rpm for 30 min. The centrifuge supernatant was not filtered and triplicate samples were placed into autosampler vials.

Chemical analysis was performed by RP-HPLC using a Waters 600E System Controller, Waters 717 plus Autosampler, and Waters 996 Photodiode Array. Samples were injected (20µl high concentration, 100µl low concentration) into Brownlee Spheri-5 RP-18 5 µm 4.6x250 mm column then eluted with a 65:35 methanol:water run in isocratic mode. The photodiode array was run in scan mode accumulating all peaks found from 230 to 400 nm for the elution time of 2,4-DNT. Each sample was analyzed in duplicate.

## 3.3 Results and Discussion

The data were evaluated using a linear adsorption isotherm expressed as:

$$C_S = K_d C_L \qquad [1]$$

where $C_S$ is the sorbed concentration (μg/g), $C_L$ is the aqueous phase concentration (μg/mL), and $K_d$ (mL/g) is the linear adsorption coefficient. Figure 4 shows a plot of the low concentration data and Figure 5 shows the high concentration data.

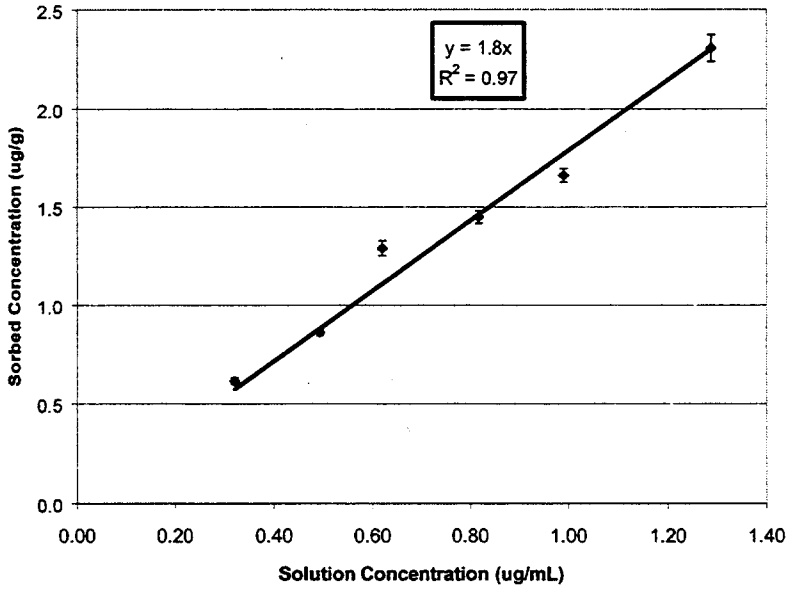


Figure 4. Low Solution Concentration Linear Adsorption Isotherm

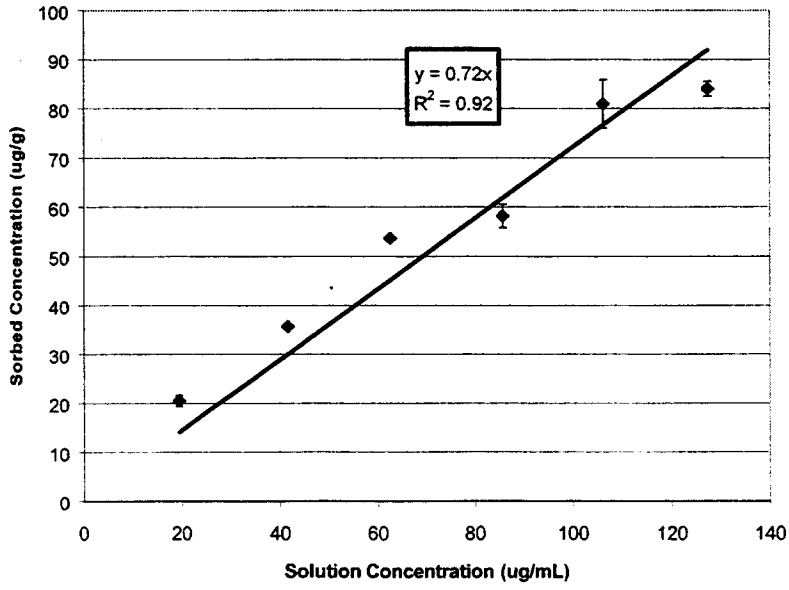


Figure 5. High Solution Concentration Linear Adsorption Isotherm

The calculated soil water partitioning coefficient derived from the slope of the line is 1.8 ($R^2$ = 0.97) for the low concentration solutions and 0.72 ($R^2$=0.92) for the high concentration solutions. The decline in the slope for the high concentration experiment implies that the sorption isotherm more likely follows a Langmuir or Freundlich model than a linear one. When fitted to a Freundlich isotherm following

$$C_S = K_f C_L^{1/n} \qquad [2]$$

where $K_f$ is the Freundlich adsorption coefficient and n is a constant, the DNT data indicate a $K_f$ = 2.1 and n = 1.3 ($R^2$ = 0.993) where $C_S$ and $C_L$ are measured in units of μg/g and μg/mL, respectively.

These data are comparable to those measured for a Midwestern soil located at Fort Leonard Wood (Pennington et al., 1999) where the mean (std dev) $K_d$ was 2.9 (1.4) mL/g.

# 4.0 Soil-Air Partitioning

## 4.1 Background

Previous work has shown that vapor solid sorption for organic chemicals is strongly impacted by the soil moisture content (Ong and Lion, 1991a and 1991b; Petersen et al., 1995 and 1996; Ong et al., 1992). For shallow buried UXO and landmines, chemical sensing of the residue of explosive chemicals in soils is being considered as a method to discriminate live from practice UXO, and locating buried landmines. The same phenomena of vapor solid sorption on dry soils may hamper UXO discrimination and landmine detection as the explosive chemicals already exhibit very low vapor phase concentrations (Phelan and Webb, 1997, 1998a and b). Past work to measure the vapor solid partitioning coefficient ($K_d$) of trichloroethylene (TCE) using a two container (with soil and without soil) concentration ratio method was successful using Brunauer-Emmett-Teller (BET) adsorption model (Peterson, et al., 1988; Ong and Lion, 1991a). Attempts to use this method were found to be infeasible due to the very low vapor densities of the explosive constituents. For TCE the vapor concentration ratio was about 1.2 (Peterson, 1988), whereas for TNT the ratio was estimated to be 1.000001, which is not measurable. The following work quantifies the moisture content dependent soil vapor partitioning phenomena for 2,4-DNT and TNT using solid phase microextraction (SPME) sampling of headspace vapors.

## 4.2 Theory

Soils are porous media with a number of physico-chemical properties that affect the transport of explosive chemicals. Soil bulk density is a measure of the compaction of the soil and is defined as

$$\rho_b = \frac{M_s}{V_s} \qquad [3]$$

where $\rho_b$ is the soil bulk density (g/cm$^3$), $M_s$ is the mass of soil particles (g), and $V_s$ is the volume of soil (cm$^3$). Soils under natural conditions have bulk densities ranging from 1.0 to 1.8 g/cm$^3$. However, soils that have been excavated and replaced, such as during the emplacement of a landmine, may have bulk densities much less than 1. The soil bulk density is inversely proportional to the soil porosity as follows

$$\phi = 1 - \rho_b / \rho_s \qquad [4]$$

where $\rho_s$ is the soil particle density (ranges from 2.6 to 2.8 g/cm$^3$ for most soils). The soil porosity, or void volume, is defined as

$$\phi = \frac{V_w + V_a}{V_s} \qquad [5]$$

where $\phi$ is the soil porosity (cm$^3$/cm$^3$), $V_w$ is the volume of soil water (cm$^3$) and $V_a$ is the volume of soil air (cm$^3$). Soil porosity values range from 0.3 for sands to 0.6 for clay rich soils. The volumetric moisture content describes how much water is present in the soil and changes greatly during precipitation/drainage events and evaporation conditions. Volumetric water content is defined as

$$\theta = \frac{V_w}{V_s} \qquad [6]$$

where $\theta$ is the volumetric water content (cm$^3$/cm$^3$). Soil moisture contents have values from near zero up to the soil porosity value. Experimental practice favors gravimetric moisture contents defined as

$$w = \frac{M_W}{M_S} \quad [7]$$

where $M_w$ is the mass of water (g). Conversion of gravimetric water content to volumetric water content is as follows

$$\theta = W \frac{\rho_b}{\rho_w} \quad [8]$$

where $\rho_w$ is the density of water (g/cm$^3$). When the soils are not fully saturated, the balance of the soil pore space not filled with water is termed the air filled porosity, and is defined as

$$a = \frac{V_a}{V_s} \quad [9]$$

where $V_a$ is the volumetric air content (cm$^3$/cm$^3$). It is often more convenient to use soil saturation ($S_L$) because it is a measure of the relative saturation of a particular soil pore space with water.

$$S_L = \frac{\theta}{\phi} \quad [10]$$

Since the explosive chemicals can exist as solutes in the soil water and the movement of soil water can be a significant transport mechanism, water solubility is an important parameter. Water solubility is defined as

$$C_L = \frac{M_{chem}}{V_w} \quad [11]$$

where $C_L$ is the concentration in aqueous phase (g/cm$^3$ soil water) and $M_{chem}$ is the mass of chemical (e.g. TNT) (g). Water solubility, however, is not constant and is typically an increasing function with temperature.

Henry's Law constant is a relative measure of the amount of the chemical that exists in the gas phase to that in the aqueous phase at equilibrium, and is defined as

$$K_H = \frac{C_G}{C_L} \quad [12]$$

where $K_H$ is the Henry's Law constant (unitless) and $C_G$ is the concentration in gas phase (g/cm3 soil gas). Henry's Law constant is also a function of temperature because both $C_G$ and $C_L$ are functions of temperature. Several groups (Dionne, 1986; Pella, 1977) have collected vapor pressure data for TNT and DNT. The data from Pella (1977) have been used in this work (Table 5).

Table 5. Vapor Pressure versus Temperature Relationships (Pella, 1977)

| Chemical | Vapor Pressure Equations |
|---|---|
| TNT | $\log_{10}(p/\text{Torr}) = (12.31 \pm 0.34) - (5175 \pm 105)\ K/T$ |
| DNT | $\log_{10}(p/\text{Torr}) = (13.08 \pm 0.19) - (4992 \pm 59)\ K/T$ |

Detailed water solubility data for DNT and TNT was used from this work as shown in Section 2. Water Solubility.

The soil partition coefficient is a relative measure of how much of the chemical is temporarily bound to the soil to that in the soil aqueous phase

$$K_d = \frac{C_S}{C_L} \quad [13]$$

where $K_d$ is the linear soil-water partition coefficient ($cm^3/g$) for water saturated soils and $C_S$ is the concentration sorbed on the soil solid phase (g/g of soil). The soil water partition coefficient is often correlated with the fraction of organic carbon found in the soils. In this way, the variability between soils can be reduced. The organic carbon distribution coefficient is defined as

$$K_{oc} = \frac{K_d}{f_{oc}} \quad [14]$$

where $K_{oc}$ is the organic carbon distribution coefficient and $f_{oc}$ is the fraction of organic carbon.

The environmental fate and transport of organic chemicals including volatilization and leaching losses has been used to explore the distribution of agricultural pesticides in soils (Mayer et al. 1974, Farmer et al. 1980, and Jury et al. 1980). These models were primarily intended to simulate specific circumstances. However, Jury et al. (1983, 1984a, 1984b, 1984c) developed and validated a general screening model (Behavior Assessment Model, BAM) that included volatilization, leaching, and degradation to explore the major loss pathways of agricultural pesticides as a function of specific environmental conditions. The Behavior Assessment Model was adapted for evaluation of chemicals in buried soils and has been termed the Buried Chemical Model (BCM)(Jury et al., 1990). This model can be used to assess the behavior of different explosive signature chemicals under particular environmental conditions and evaluate the potential for chemical signature discrimination of landmines and UXO.

The formulations of the BAM and BCM models begin by defining phase partitioning phenomena. These are valuable in that they can express the total concentration of a chemical in the gas, aqueous and sorbed phases. The total concentration is expressed as

$$C_T = \rho_b C_S + \theta C_L + a C_G \quad [15]$$

where $C_S$ is the concentration sorbed to the soil, $C_L$ is the solute concentration in the aqueous phase, and $C_G$ is the gas phase concentration. In addition, Jury (1983) shows how equation [15] can be rewritten in terms of one of the variables alone

$$C_T = R_S C_S = R_L C_L = R_G C_G \quad [16]$$

where

$$R_S = \rho_b + \frac{\theta}{K_d} + a\frac{K_H}{K_d} \quad [17]$$

$$R_L = \rho_b K_d + \theta + a K_H, \text{ and} \quad [18]$$

$$R_G = \rho_b \frac{K_d}{K_H} + \frac{\theta}{K_H} + a \quad [19]$$

are the solid, liquid and gas phase partition coefficients, respectively.

In their evaluation of vapor phase transport in soils, Ong et al., 1992, added vapor-solid sorption such that equations [15] and [16] become

$$C_T = \theta C_L + aC_G + C_L K_d \rho_b + C_G K_{SG} \rho_b \quad [20]$$

and

$$C_T = R_S C_S = R_L C_L = R_G C_G = R_{SG} C_{SG} \quad [21]$$

where

$$R_L = \rho_b K_d + \theta + aK_H + \rho_b K_H K_{SG} \quad [22]$$

$$R_G = \rho_b \frac{K_d}{K_H} + \frac{\theta}{K_H} + a + \rho_b K_{SG} \quad [23]$$

$$R_{SL} = \rho_b + \frac{\theta}{K_d} + a\frac{K_H}{K_d} + \frac{\rho_b K_H K_{SG}}{K_d}, \text{ and} \quad [24]$$

$$R_{SG} = \frac{\rho_b K_d}{K_H K_{SG}} + \frac{\theta}{K_H K_{SG}} + \frac{a}{K_{SG}} + \rho_b \quad [25]$$

are the liquid, gas and solid-liquid and solid-gas phase partition coefficients, respectively.

This formulation introduces a new term, $K_{SG}$ that is a function of the overall vapor solid partition coefficient ($K_{d'}(w)$), which is highly dependent on the soil moisture content. $K_{SG}$ is defined as (Ong et al., 1992)

$$K_{SG} = K_{d'}(w) - \frac{K_d}{K_H} - \frac{w}{100 K_H \gamma \rho_w} \quad [26]$$

where

$$K_{d'}(w) = \frac{C_S}{C_G} \quad [27]$$

and $w$ is the gravimetric moisture content (g/g), $\gamma$ is the activity coefficient for the solute in the soil water (approximates 1 for a dilute solution), and $\rho_w$ is the density of water (g/cm$^3$). Note that equation [26] in Ong et al. (1992) has an incorrect sign on the last term (Webb et al., 1999). Petersen et al. (1995) has defined an equation for $K_{d'}(w)$ as an exponential function described by

$$A = \log(K_{d'}(w)) \quad [28]$$

$$A = (A_0 - \beta(w))e^{-\alpha \cdot w} + \beta(w) \quad [29]$$

$$\beta(w) = \log\left(\frac{K_d}{K_H} + \frac{w}{K_H \gamma \rho_w}\right) \qquad [30]$$

where, $A_0$ is the log $K_d$, at zero moisture content and alpha is a fitting parameter describing the curvature of the non-linear part of the relationship. Equation [29] can be fit with non-linear regression analysis to provide estimates for $A_0$ and alpha. In equation [29], the first term describes the non-linear region and the second term describes the linear region. Ong et al., 1990, characterize the vapor-solid partitioning in the linear region as being controlled by Henry's Law Constant ($K_H$). This is because there is sufficient water in the system that the vapor must first partition into the soil water prior to partitioning onto the soil particle. In the non-linear portion, sorption sites previously occupied by water become available for sorption of DNT or TNT.

Both Petersen (1995) and Ong and Lion (1991a) compared the moisture content at which the $K_d$(w) became exponential for several soils and was found to be at about 4 to 5 monomolecular layers of water. The moisture content at integer number monomolecular layers of soil water is a function of the soil specific surface area and is described by

$$w_x = x\left(\frac{S_A MW_w}{MA_w A_n}\right) \qquad [31]$$

where, x=1,2,3... is the number of monolayers, $S_A$ is the specific surface area of the soil ($m^2/g$), $MW_W$ is the molecular weight of water (18 g/mol), $MA_W$ is the molecular area of water (1.15e-19 $m^2$/molecule), and $A_N$ is Avogadro's number (6.02e-23 molecules/mole). The specific surface area ($S_A$) of soils range from 10 $m^2/g$ for sand to 100's $m^2/g$ for some types of clay. Figure 6 shows the correlation of

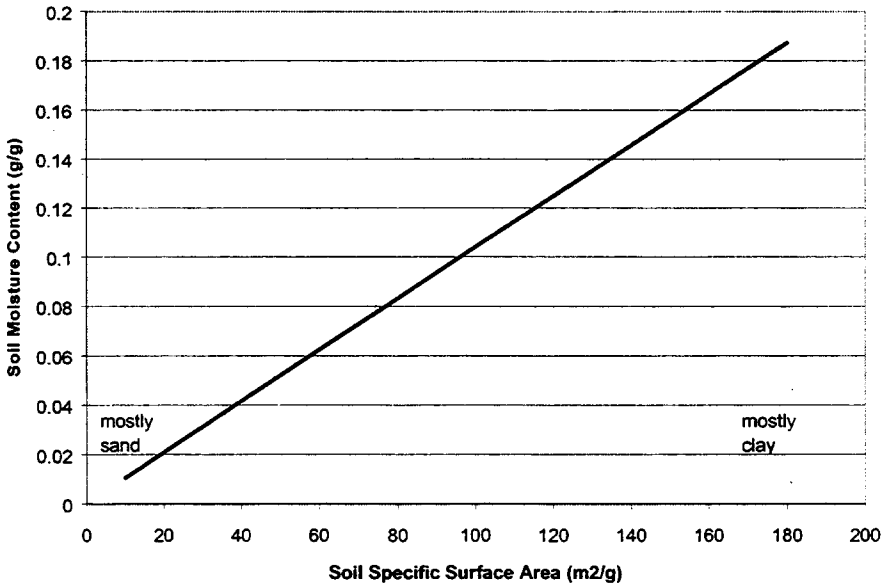


Figure 6. Moisture Content at Four Monomolecular Layers of Water

soil specific surface area to the moisture content at four monomolecular layers of water. The proportion of clay in soils strongly influences the soil specific surface area due to the small size of the clay soil particles.

In their evaluation of toluene and trichloroethene, $K_d$ increased about $10^4$ from the point of four monomolecular layers to oven dry soil moisture contents (Petersen, 1995; Ong and Lion, 1991a).

In the evaluation of performance requirements for sampling and analysis alternatives, one can more easily find soil residue values and use the partitioning equations above to estimate the vapor concentrations in equilibrium with that soil. For surface soils, vapors in the boundary layer can be assumed to be equivalent to the soil gas concentration ($C_G$) within the soil pores. A soil sample for explosive constituents can be considered to be the total concentration in the soil ($C_T$). With data for $\rho_b$, $\theta$, $K_H$, $K_d$ and $K_d$(w), the $C_G$ can be estimated from equations [21] , [23], [26] through [30].

## 4.3 Materials and Methods

*Soil Preparation*

The same source of soil as that used for the soil-water partitioning tests (section 3.2) were used for the soil-air partitioning tests. This soil was screened to collect the less than 2 mm fraction and dried in an oven at 140°C for seven (7) days. Analytical grade DNT crystals were added to the soil in a one (1) gallon paint can to a concentration of about 10 mg/kg. The paint can was placed on a rock tumbler for 4 days at about 30 rpm. Water was added to bring the soil to about 0.01 g water/g soil, then placed in an oven at 110°C for 4 days to distribute the DNT and water as evenly as possible. The paint can was removed from the oven and placed on the rock tumbler for one (1) day. To create a lower soil concentrations, the stock soil was serially diluted 1:10 with clean dry soil. Recrystallized military grade TNT was used to prepare TNT doped soil in a similar fashion to a concentration of about 100 mg/kg.

*Analytical Methods*

Ten (10) soil samples (~0.8 gram) were collected from the top surface of the stock DNT and TNT paint cans. The soils were extracted with 5:1 soil to acetonitrile in water temperature cooled (15°C) ultrasonic bath for 16 hours. The extracts were filtered with a 0.45 um nylon syringe filter. Quantitation was performed with a 1 µL injection into a HP 6890 Gas Chromatograph equipped with a micro electron capture detector and a 0.53mm x 6 m RTX 225 0.1 um film thickness column. The split/splitless injector was programmed for a 220°C inlet temperature, starting column temperature of 100°C for 2 minutes, ramped to 200°C at 10°C/min, then held for 7 minutes. The splitter opened 45 seconds after sample injection. The SPME fibers were analyzed on the same GC system with manual injection. Five (5) soil samples were collected to measure BET surface area using a Micromeritics Accelerated Surface Area and Porosimetry 2405 Instrument that measures BET surface area with $N_2$.

*SPME Calibration*

The SPME fibers (Supleco, 65 µm PDMS/DVB) were calibrated using the methods developed by Jenkins et al., 1999. This method measures the amount of analyte sampled by the SPME fiber per unit time and estimates the effective sampling rate from the assumed vapor density as follows:

$$EVSR_{SPME} = \frac{MSR_{SPME}}{VD_T} \qquad [32]$$

where, the $EVSR_{SPME}$ is the Effective Volumetric Sampling Rate (mL/min) for the SPME, the $MSR_{SPME}$ is the Measured Sampling Rate (pg/min) for the SPME in the headspace volume, and the $VD_T$ is the assumed vapor density (pg/mL) at the measured temperature. For both DNT and TNT we use the vapor pressure data from Pella, 1977 (Table 5).

About 100 mg of DNT or TNT was placed into a 40 mL amber septa top vial and left to equilibrate on the lab benchtop or in a temperature controlled water bath. SPME fibers were placed into the headspace for 1 minute. Temperature was measured with a thermocouple sensor held in the air or water adjacent to the calibration vial.

*Headspace Measurement*

To begin the tests, ~1 gram of soil was placed into a 5 dram amber, septa top vial. Ten (10) or five (5) vials were prepared for each trial. SPME fibers were used to sample the headspace vapor by placement into the headspace and allowed to equilibrate for 15 to 1000 minutes, sufficient to collect enough mass to be quantified. All ten or five vials were sampled simultaneously, then analyzed within 4 hours. Deionized water was then added to each vial (5, 10 or 20 uL), the vial was shaken briefly, then allowed to equilibrate for at least 18 hours. The SPME sampling and analysis was then repeated and another aliquot of deionized water was added to each vial. Table 6 shows the vials designations and aliquots of water used.

Table 6. Sequential Quantity of Water Added

| Vial | Source | Incremental Water Added (uL) |
|---|---|---|
| DNT: 1-10 | Stock | 20, 20, 20, 20, 20 |
| DNT: I-X | Stock | 5, 5, 5, 5, 5, 5 |
| DNT: A-F | 1:10 Dilution | 10, 10, 10, 10, 10, 10, 20, 20 |
| TNT: 1-10 | Stock | 10, 10, 10, 10, 10, 10, 10, 10, 10, 10 |

The headspace vapor concentration was determined as follows:

$$C_G = \frac{M_{SPME}/T}{EVSR_{SPME}} \qquad [33]$$

where $M_{SPME}$ is the mass measured on the SPME fiber and T is the sampling time. At the end of each experiment, half of the vials were sacrificed for moisture content and half were sacrificed for acetonitrile extractable DNT or TNT.

## 4.4 Results and Discussion

Calibration of the effective sampling rate for the SPME was performed periodically through the test. Figure 7 shows the effective sampling rate as a function of temperature for DNT. This sampling rate increases with temperature; however, the correlation is not very good. Figure 8 shows the effective sampling rate for TNT, which has significantly more random error.

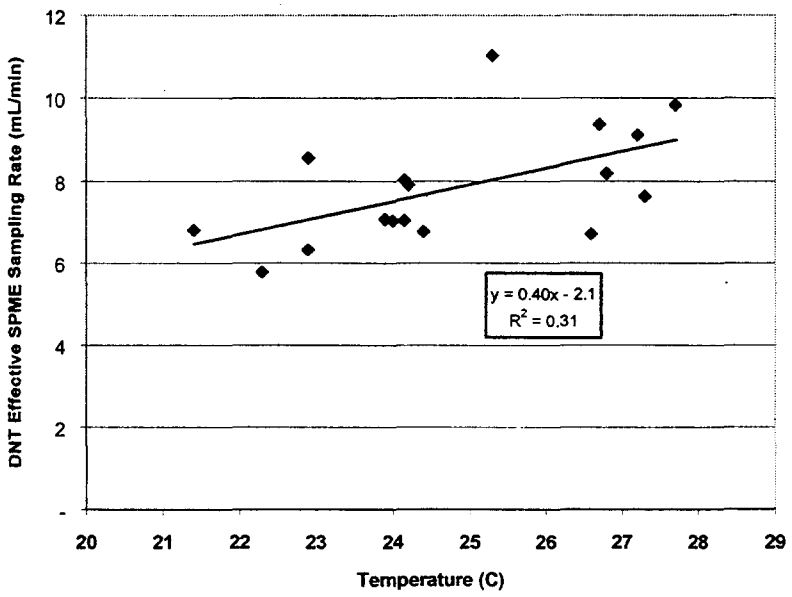


Figure 7. DNT SPME Effective Sampling Rate vs. Temperature

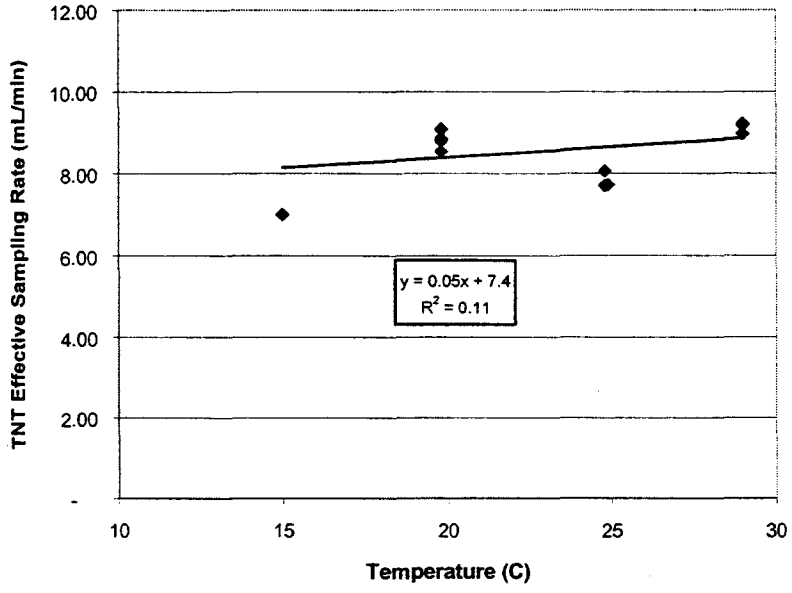


Figure 8. TNT SPME Effective Sampling Rate vs. Temperature

Table 7 shows the mean and standard deviations of the initial pre-test DNT and TNT soil concentrations and soil moisture contents. The BET surface area of the stock DNT soil showed a mean value (std. dev.) of 23 $m^2/g$ (0.3) n=5.

Table 7. Pre-Test DNT and TNT Mean Soil Concentration and Soil Moisture Content

| Source | Soil Concentration (ug DNT/kg dry soil) mean (stdev) n | Soil Moisture Content (g water/g dry soil) mean (stdev) n |
|---|---|---|
| Stock DNT Soil | 6895 (628) 10 | 0.0112 (0.0016) 2 |
| 1:10 Diluted DNT Soil | 676 (30) 3 | 0.0112 (0.0016) 2 |
| Stock TNT Soil | 99,927 (4168) 10 | 0.0041 (0.0002) 3 |

Figure 9 shows the DNT headspace concentration for the stock and 1:10 diluted soil sets. Since there was significant uncertainty in the effective SPME sampling rate as a function of temperature, a single sampling rate of 7 mL/min for DNT and 8.5 mL/min for TNT was used. The average (std dev) temperature for all of the DNT tests was 23.0 (0.7) °C and for TNT was 22.6 (0.7) °C. For the sampling and analysis method used, a 100 min SPME sample time with a 1 pg GC/ECD detection limit, the lower limit of determination for DNT is about 0.001 ng/L. Data at the 0.01 and 0.02 g/g moisture contents were highly uncertain with many of the measurements found to be non-detectable.

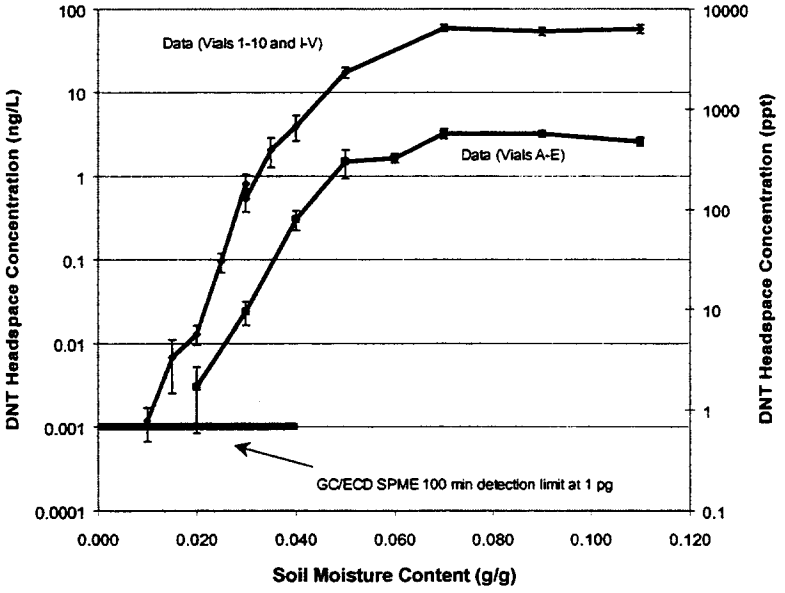


Figure 9. DNT Soil Headspace Concentration versus Soil Moisture Content

Figure 10 shows the data for the single set of vials with TNT.

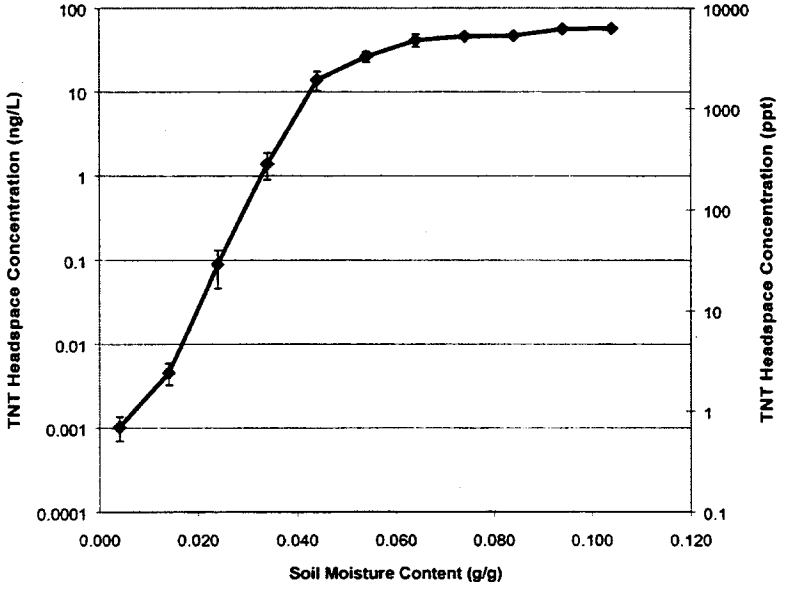


Figure 10. TNT Soil Headspace Concentration versus Soil Moisture Content

Table 8 shows the post-test mean soil DNT and TNT concentrations and soil moisture contents. The DNT soil concentrations found in Vials 6-10 appeared very low compared to pre-test conditions (Table 7) and post-test Vials I-V. A review of the analytical data show no unusual aspects. The moisture contents for all vials indicated about 20% lower values than the amount of water added during the test series. Moisture loss through repeated penetration of the septum may be one explanation. All calculations were performed with the applied water volume rather than back calculated actuals from the post-test moisture analyses. To establish Kd' values, the average of the pre and post-test DNT soil concentrations were used, with the exception that only the pre-test values were used for Vials 6-10 due to the anomalous post-test Vial 6-10 data.

Table 8. Post-Test DNT and TNT Mean Soil Concentration and Soil Moisture Content

| Source | Soil Concentration (ug DNT/kg dry soil) mean (stdev) n | Source | Soil Moisture Content (g water/g dry soil) mean (stdev) n |
|---|---|---|---|
| DNT: Vials 6-10 | *1063 (355) 5 | Vials 1-5 | 0.090 (0.007) 5 |
| DNT: Vials A-E | 650 (57) 4 | Vials F-J | 0.085 (0.007) 4 |
| DNT: Vials I-V | 6540 (213) 5 | Vials VI-X | 0.032 (0.001) 5 |
| TNT: Vials 1-5 | 98874 (5274) 5 | Vials 6-10 | 0.135 (0.010) 5 |

* - anomalous low values

Figure 11 illustrates the DNT $K_{d'}(w)$ for both soil concentrations. The vapor phase concentrations were those as measured (Figure 9) and the soil concentrations were an average of the pre- and post-test values (not using post-test vials 6-10). Figure 12 shows the $K_{d'}(w)$ as a function of the monomolecular layers of water coverage using equation [31]. These experimental results indicate a moisture content consistent with ten (10) monomolecular layers of water where the $K_{d'}(w)$ begins the exponential rise, compared with five (5) reported by Ong and Lion, 1991a. Figure 13 shows the $K_{d'}(w)$ for TNT.

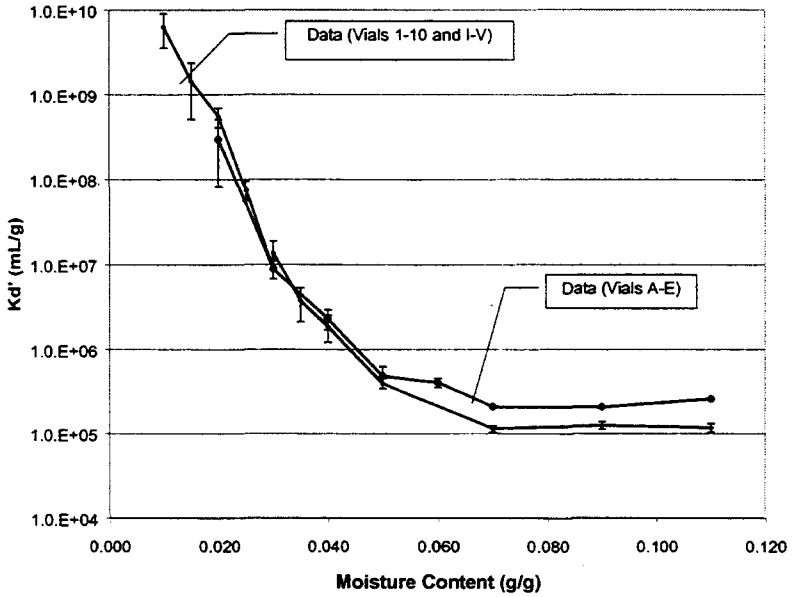


Figure 11. DNT Soil Vapor Partitioning Coefficient ($K_{d'}$) as a Function of Moisture Content (w).

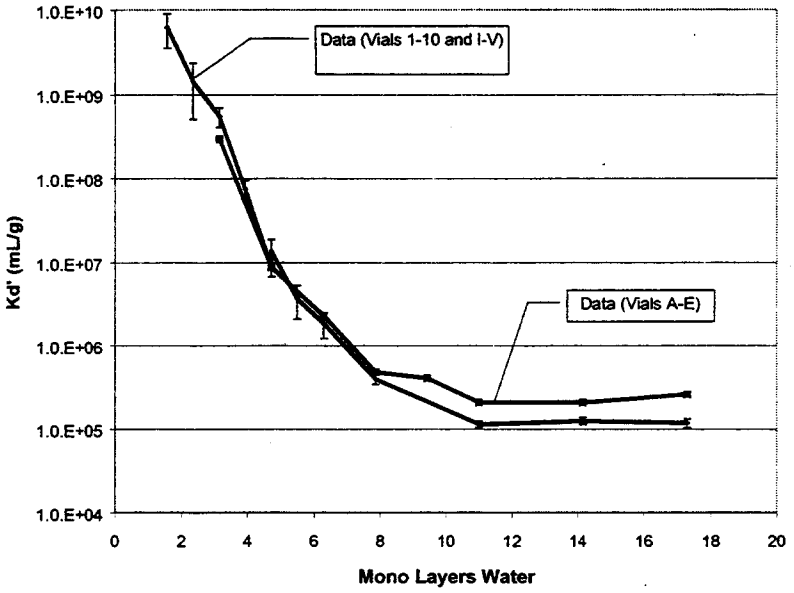


Figure 12. DNT Soil Vapor Partitioning Coefficient ($K_{d'}$) as a Function of Mono Layers of Water

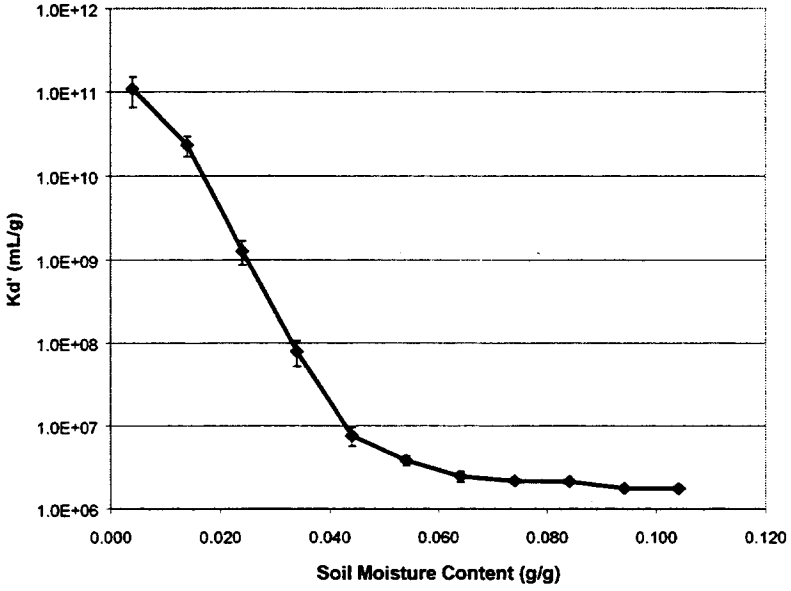


Figure 13. TNT Soil Vapor Partitioning Coefficient ($K_{d'}$) as a Function of Moisture Content (w).

Using a non-linear curve fitting routine (weighted non-linear least squared regression, Marquardt-Levenburg algorithm, SPSS Sigma Stat Ver. 2.3), the parameters $A_0$ and $\alpha$ were estimated from equation [29] and [30]. These values were placed into equations [28] through [30] with a DNT $K_d$ =1.8 mL/g (see Section 3, consistent with a low soil water solute concentration) and a temperature of 23°C which equates to a $K_H$ = 8.72e-6 to produce the model values of $K_{d'}(w)$. Instead of using four monolayers water coverage to initiate the non-linear part of the $K_{d'}(w)$, a ten monolayer model was used to be consistent with the data as shown in Figure 12. Figure 14 shows the model fit and parameter estimates for the combined DNT data (all vials).

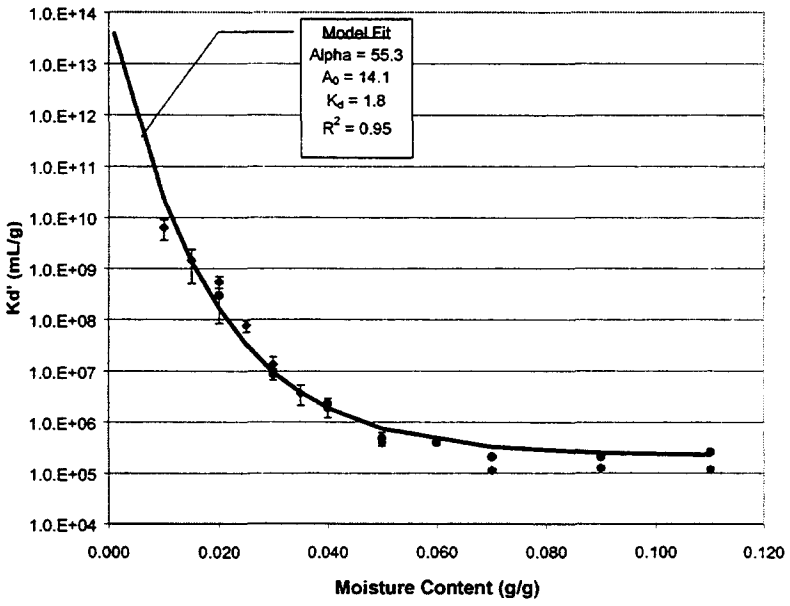


Figure 14. DNT Parameter Estimation for All Vials with a Fixed $K_d$

In Figure 14, the non-linear portion of the curve appears to have a good visual fit. However, the linear portions appear to predict somewhat high. Figure 15 illustrates the parameters that influence various portions of the curve. In the linear area at high moisture contents, it is the ratio of $K_d/K_H$ that is important.

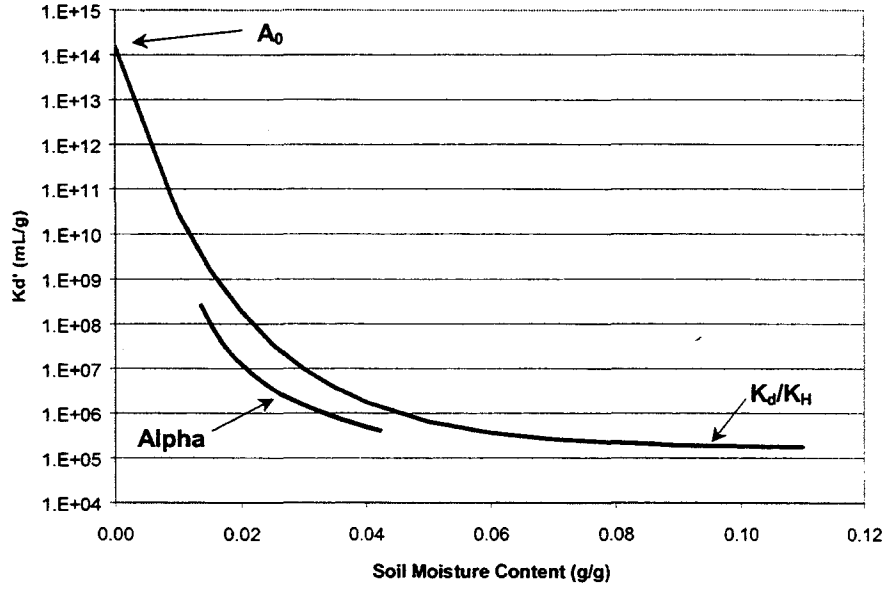


Figure 15. Generic Relationships of $K_{d'}(w)$

With uncertainties in the values for $K_d$ with DNT, the non-linear regression analysis was performed as before, allowing $K_d$ to be a fitting parameter in addition to alpha and $A_0$ for the combined DNT data set. Figure 16 shows the results of the fitting exercise with revised estimates

of alpha, $A_0$ and $K_d$. The $K_d$ estimate is about 30% of the measured $K_d$ from the low range solutions.

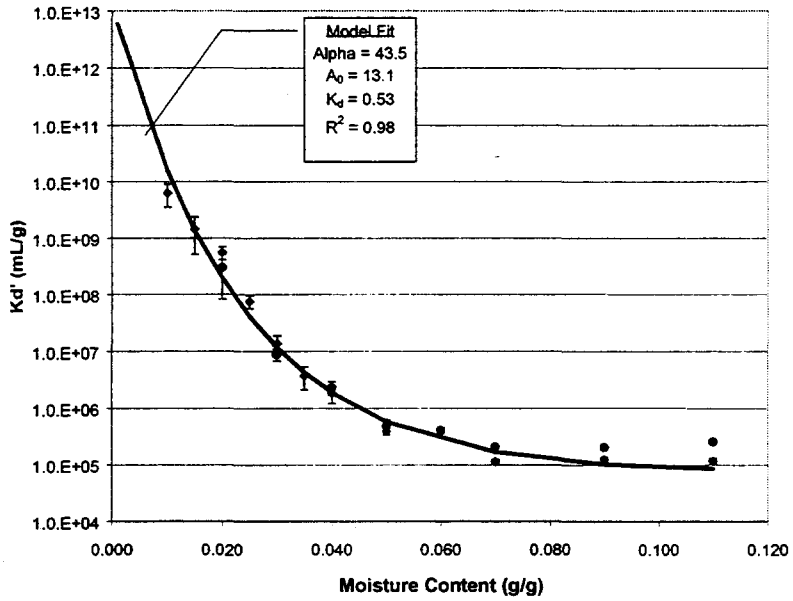


Figure 16. DNT Parameter Estimation for all Vials using $K_d$ as a Fitting Parameter

The $K_d$ value used in the model predictions in Figure 14 was 1.8 mL/g based on equilibrium solution concentrations of 0.3 to 1.3 ug/mL. For the soils containing 6718 and 663 ng/g DNT (the average of the pre- and post-test soil extraction samples), the soil water would contain 3.7 and 0.37 ug/mL DNT using a $K_d$ of 1.8 mL/g, respectively. These estimated soil water concentrations are near the range for the low range $K_d$ measurements (Section 3) supporting the $K_d$ value of 1.8 mL/g. However, Figure 16 indicates that the $K_{d'}(w)$ data would better support a lower $K_d$ of 0.5 mL/g consistent with the higher range batch equilibrium $K_d$ = 0.7 mL/g. Similar differences in $K_d$ values have been noted with dynamic soil column breakthrough tests (Phelan et al., 2000).

Overestimation of soil-water partition coefficients using batch equilibrium measurement methods has been reported (Burglsser et al., 1993) as a result of the particle concentration effect (solid-to-solution ratio and increased sorption capacity caused by particle separation during soil preparation).

Measurement of the soil-water partition coefficient for TNT was not completed as part of this effort. However, Pennington and Patrick (1990) report batch equilibrium linear $K_d$ values for TNT from thirteen soils found at Army Ammunition Plants with values from 2.5 to 6.8 mL/g. An estimate of the $K_d$ value for TNT was included in a non-linear regression parameter estimation for the TNT $K_{d'}(w)$ data, where $K_H$ was fixed at 6.98e-7 (23°C). Figure 17 shows the data model comparisons and parameter estimates (without using the $K_{d'}$ data for moisture content of 0.4% (g/g) as the data appeared to be below the method quantitation limit). The $K_d$ value of 0.9 mL/g is consistent with other reports that TNT typically has higher values than DNT.

Figure 18 shows a summary of both the DNT and the TNT $K_{d'}(w)$ data/model comparisons with parameter estimates that will be used in forthcoming analyses.

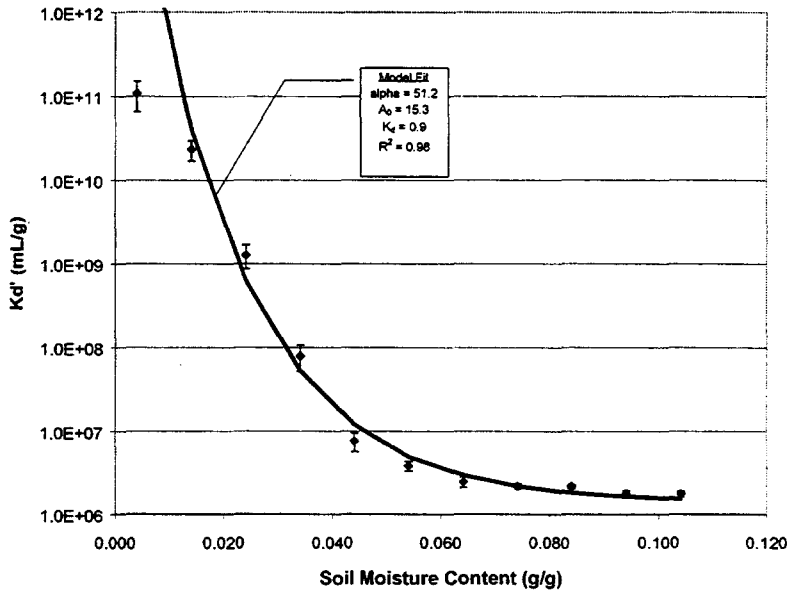


Figure 17. TNT Parameter Estimation using $K_d$ as a Fitting Parameter

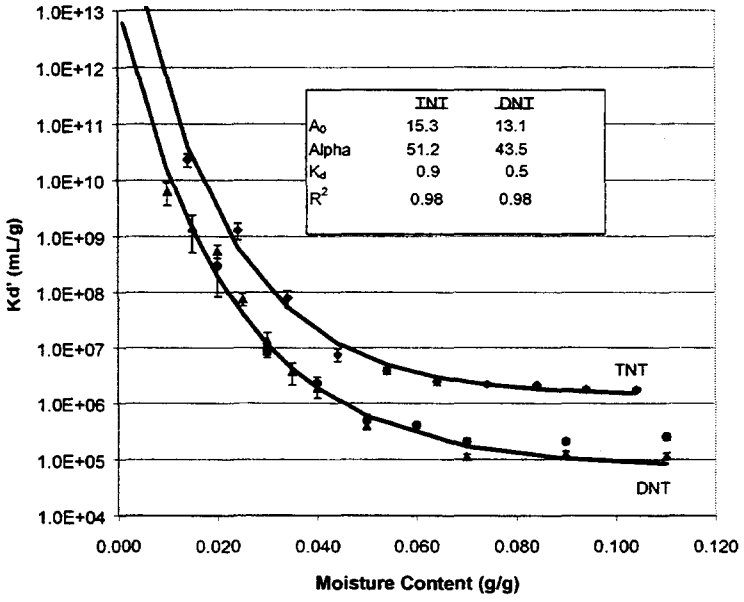


Figure 18. DNT and TNT Data Model Comparisons

Figure 18 shows the combined results of three data sets; two for DNT with $C_T$ that varies by about 10 and one for TNT that was greater than the high DNT by a factor of about 15. The validity of the $K_{d'}(w)$ relationship to other total soil concentrations ($C_T$) is needed in order to make broader extrapolations. This was evaluated by making decade dilutions of the DNT and TNT stock soils with clean dry soil. Five decades of soil residues containing TNT were planned for 100, 10, 1, 0.1, 0.01 μg/g (jars 1-5). The DNT soil residues were similarly planned for 6, 0.6, 0.06, 0.006 and 0.0006 μg/g (jars 6-10) to create headspace vapor concentration of similar magnitude as the TNT. Three (3) soil samples (~0.8 gram) were collected from the top surface of the each DNT and TNT soil standard and analyzed as noted previously.

Table 9 shows the results from the samples obtained from the decade dilution and stock soil standards. This shows that the serial dilution method of creating decade lower concentrations is a viable technique for the soils.

Table 9. Decade Dilution Soil Residue Results, μg/g (n=3)

| Jar | TNT | | 2,4-DNT | |
|---|---|---|---|---|
| | Avg | Std Dev | Avg | Std Dev |
| 1 | 105 | 2.8 | | |
| 2 | 9.7 | 0.6 | | |
| 3 | 0.94 | 0.1 | | |
| 4 | 0.39 | 0.02 | | |
| 5 | 0.07 | 0.003 | | |
| | | | | |
| 6 | | | 5.9 | 0.40 |
| 7 | 0.05 | 0.001 | 0.58 | 0.04 |
| 8 | 0.17 | 0.010 | 0.05 | 0.005 |
| 9 | 0.50 | 0.002 | 0.006 | 0.002 |
| 10 | 0.16 | 0.010 | <MDL | |

MDL – minimum detection limit

Unfortunately, the clean soil used to make the dilutions contained a small residue of TNT that appeared to be quite variable. Three samples of the clean soil showed an average of 0.04 μg/g. However, Table 9 shows levels up to 0.50 μg/g (Jar 9) and Jar 4 had about 0.30 μg/g more than estimated from dilution from Jar 3.

Under dry soil conditions, the highest soil residues prepared would be marginally detectable using the SPME sampling system. However, when wetted, the headspace vapor concentrations are much greater. Figure 19 shows the expected vapor concentrations from both the DNT and TNT soil standards using equation [21] and the parameters shown in Figure 18.

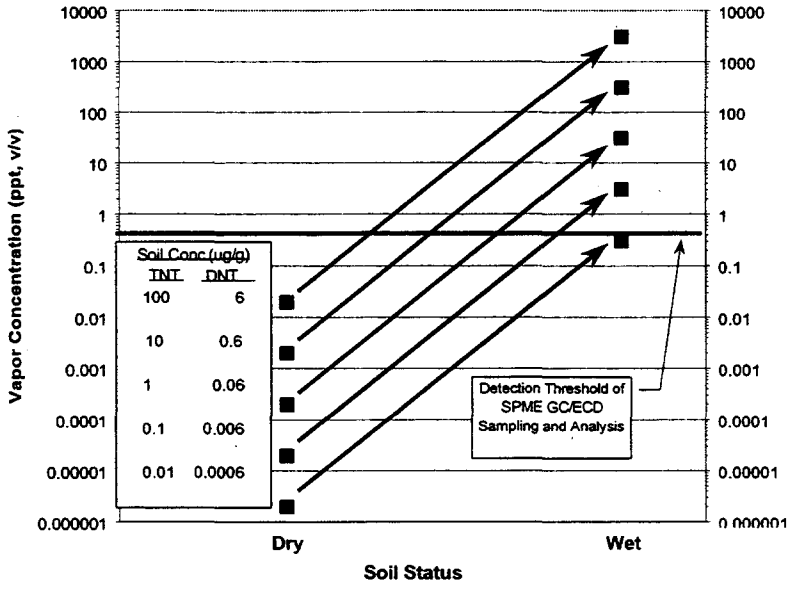


Figure 19. Expected Vapor Concentrations for Decade Dilutions of DNT and TNT Soil Standards

A 100 g aliquot of each soil standard was placed into a 250 mL jar fitted with a septum screw cap top. Ten (10) mL of tap water was pipetted into each jar to bring the soil moisture up to 0.10 g/g. The jar was shaken for 1 minute followed immediately by SPME headspace sampling of various duration to achieve instrument detection thresholds. Table 10 shows the results of the headspace samples.

Table 10. Decade Dilution Jar Headspace Concentrations

| Jar | Dry/ Wet | SPME Time (min) | TNT (pg/mL) | 2,4-DNT (pg/mL) | TNT (ppt) | 2,4-DNT (ppt) |
|---|---|---|---|---|---|---|
| 1 | Dry | 100 | | | | |
| 1 | Wet | 10 | 24.2 | | 2612 | |
| 2 | Wet | 30 | 2.5 | | 268 | |
| 3 | Wet | 60 | 0.19 | | 20 | |
| 4 | Wet | 100 | 0.08 | | 9 | |
| 4 | Wet | 960 | 0.34 | | 37 | |
| 5 | Wet | 100 | 0.02 | | 3 | |
| 5 | Wet | 960 | 0.01 | | 1 | |
| | | | | | | |
| 6 | Dry | 100 | | 0.003 | | 0.4 |
| 6 | Wet | 10 | | 33.9 | | 5280 |
| 7 | Wet | 30 | | 3.1 | | 486 |
| 8 | Wet | 60 | | 0.28 | | 43 |
| 9 | Wet | 100 | | 0.03 | | 4 |
| 9 | Wet | 960 | | 0.06 | | 9 |
| 10 | Wet | 100 | | 0.004 | | 0.6 |
| 10 | Wet | 960 | | 0.005 | | 1 |

As expected, Jars 1 and 6 under dry conditions had barely detectable analyte levels; however, under wet conditions, the headspace concentrations appear to follow the decade dilutions. These headspace concentrations were about 35 to 50 percent less than estimated from equation [21]. An analysis of the kinetics of vapor release may partially explain this phenomenon for DNT, but not for TNT (see section 4.5). Figures 20 and 21 show the correlation of soil residue to soil headspace concentration for DNT and TNT, respectively

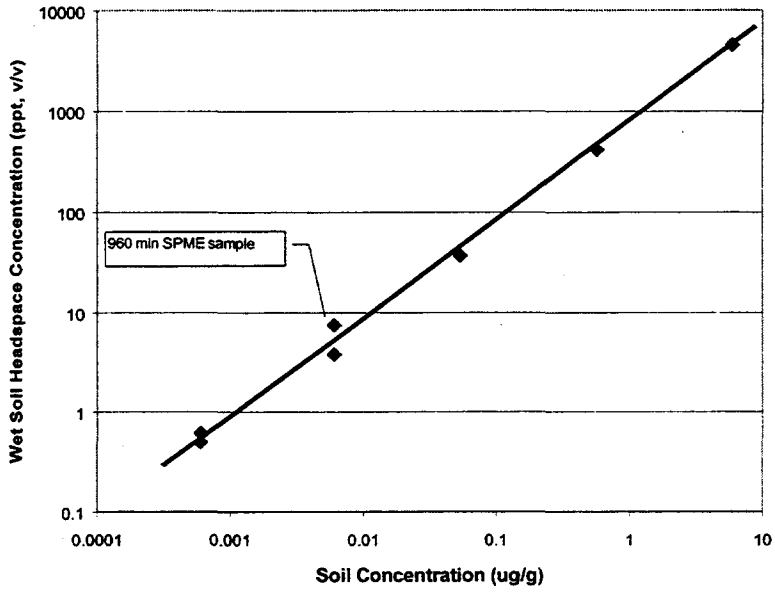


Figure 20. DNT Soil Residue vs Soil Headspace Concentration

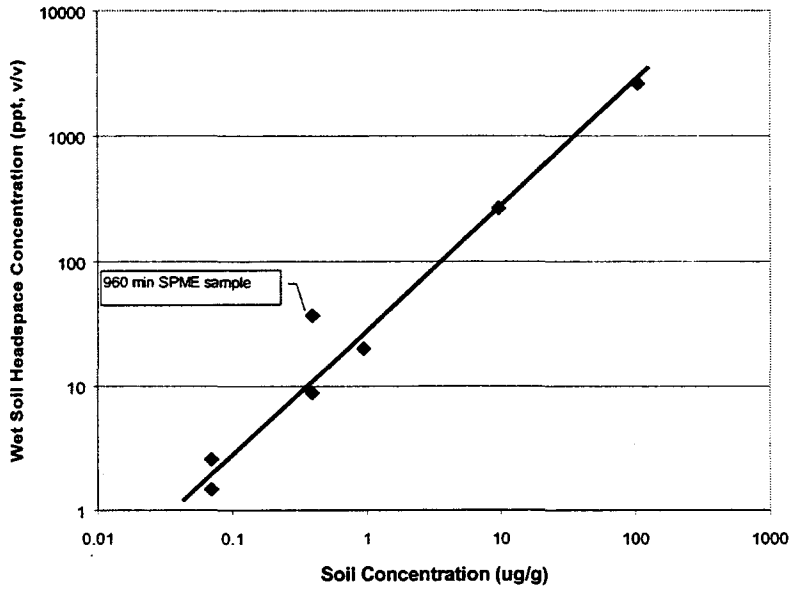


Figure 21. TNT Soil Residue vs Soil Headspace Concentration

For the second lowest dilution soil residues for DNT and TNT, longer headspace SPME sampling (960 min vs 100 min) showed a upward bias (factor of 2-4) in the calculated vapor concentration. These long sampling times may be unreliable as the sampling rate calibration was based on much shorter time intervals. For the lowest soil dilution, both the long and the short SPME samples were similar; however, both were less than 10 times the instrument detection limit. These correlations show that extrapolation of $K_{d'}(w)$ to lower total soil residues is not unreasonable over a range of $10^3$ to $10^4$.

One reason why this correlation might be valid in this range is that there is much less than a monolayer coverage of the DNT or TNT on the soil surfaces. Molecular modeling estimates of the dimensions of TNT and DNT are shown in Table 11 (MSI Insight Molecular Modeler).

Table 11. Molecular Dimensions of DNT and TNT (Angstroms)

| | x | y | z |
|---|---|---|---|
| DNT | 9.437 | 8.317 | 3.754 |
| TNT | 9.514 | 9.958 | 3.754 |

If the TNT lays planar to the soil surface there will be about $1.05 \times 10^{18}$ molecules/$m^2$. This equates to about $4 \times 10^{-4}$ g/m2, which on a soil with an average surface area of 23 $m^2$/g, equates to a soil residue of 9 mg-TNT/g-soil. The highest TNT levels used in this study were 90 times less than a single monolayer coverage.

## 4.5 Kinetics

To evaluate the kinetics of chemical release from soil by adding water, a test was performed using the DNT stock and the TNT stock (see Table 7). The same soil and vial setup was used as for the steady state measurements (~1 gram soil in a 5 dram vial) and 100 µl of water was injected through the septum to bring the soil up to a moisture content of 0.10 g/g. The vial was shaken for 1 minute. Then ten (10) minute SPME samples were collected ending at 10, 20, 40, 70, 140, 280, 1560, 2980, 7440, 8890 and 10220 minutes after water was added and shaken. DNT and TNT headspace concentrations were derived from the mass accumulated on the SPME and a sampling rate of 7 mL/min for DNT and 8.5 mL/min for TNT (eq. [33]). Figure 22 shows the results from three replicate vials for DNT.

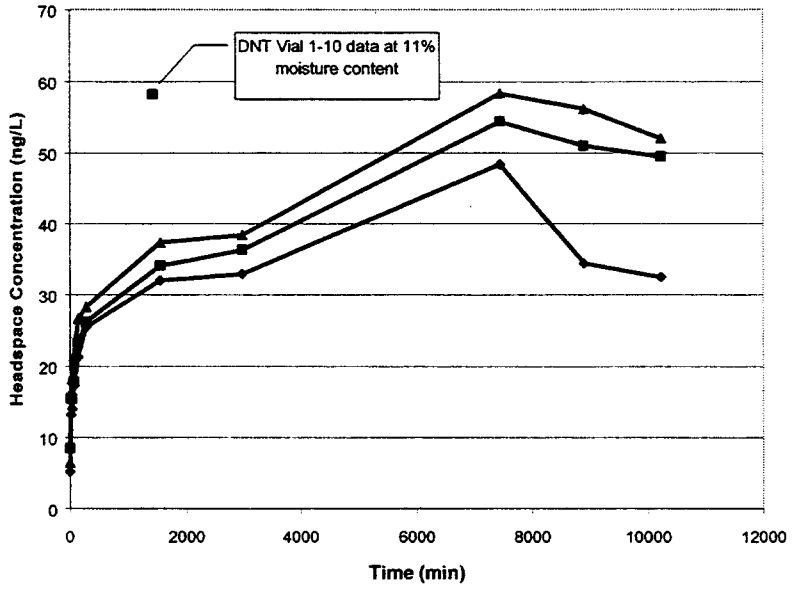


Figure 22. DNT Vapor Release Kinetics

The DNT headspace vapor levels rises quickly (300 min.) up to about half the steady state concentration. Peak levels are reached in about 8000 minutes and are nearly the same magnitude as the peak concentration rising with incremental water addition (see Figure 9, Vials 1-10). Declines from peak vapor concentrations may be due to degradation of the DNT in the wet soils.

Figure 23 shows the results for the TNT replicates. These results show an enhanced vapor induction of about a factor of three over the incremental water addition peak concentration (see Figure 10). These peak levels are reached at the end of 20 minutes. The vapor levels then fall back to about the steady state level after about 2000 minutes. This behavior is very different than that of the DNT and no explanation is offered. However, SPME sampling during this transient period of vapor release may be a partial reason for the lower than expected values for DNT, but is contrary for TNT, during the decade dilution tests (Table 10) noted above.

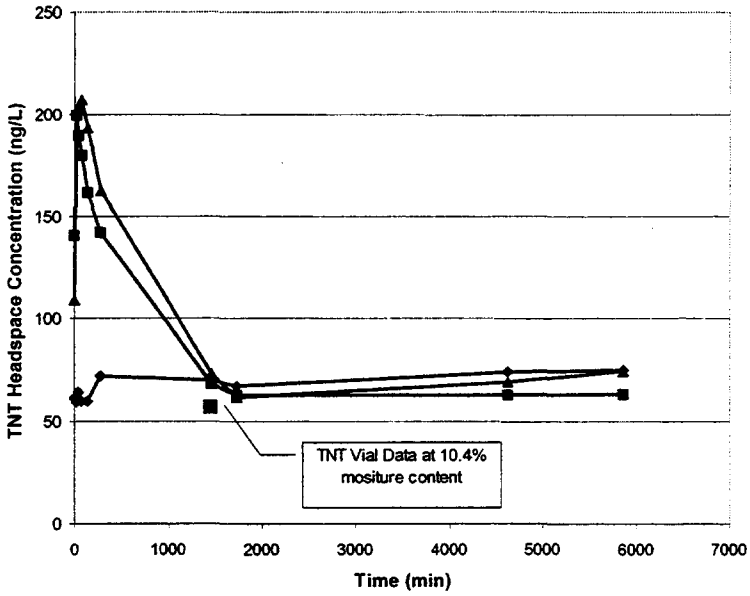


Figure 23. TNT Vapor Release Kinetics

# 5.0 Integrated Soil System Phase Partitioning

The relationships described in section 4.2 through 4.4 can be assembled to show the phase partitioning relationships between the sorbed, liquid and gas phases. One can then evaluate shifts in these relationships due to changes in some of the key parameters. Jury et al. (1991) showed how the phase partitioning coefficients (eq. [16]-[19]) could be defined as phase mass fractions as follows:

$$f_S = \frac{\rho_b C_S}{C_T} \quad [34]$$

$$f_L = \frac{\theta C_L}{C_T} \quad [35]$$

$$f_G = \frac{a C_G}{C_T} \quad [36]$$

where $f_S$ is the mass fraction sorbed to the soil, $f_L$ is the mass fraction in the aqueous phase, and $f_G$ is the mass fraction in the gas phase. By definition,

$$f_S + f_L + f_G = 1 \quad [37]$$

Table 12 and 13 shows a copy of a spreadsheet with integrated equations for the phase partitioning of TNT and DNT, respectively.

These spreadsheets can be used to evaluate impacts of various input parameters on the phase specific concentrations and mass fractions. Figure 24 shows an example of the soil solid and liquid phase mass fraction of TNT and DNT using the input parameters shown in Table 12 and 13. At all soil saturations, DNT always has a greater liquid mass fraction and a lower sorbed mass fraction when compared to TNT. The liquid phase mass fraction rises as more water is present in the soil pore space. When the saturation drops below about eight percent, the impact of the vapor-solid partitioning process becomes evident. The liquid phase mass fraction becomes negligible with most of the mass fraction sorbed to the solid phase.

Table 12. TNT Phase Partitioning Estimation Spreadsheet

| Parameter [equation] | | Value | Units |
|---|---|---|---|
| soil bulk density - $\rho_b$ | [3] | 1 | g/cm$^3$ |
| soil particle density - $\rho_s$ | | 2.6 | g/cm$^3$ |
| soil porosity - $\varphi$ | [4] | 0.62 | cm$^3$/cm$^3$ |
| soil moisture (vol) - $\theta$ | [6] | 0.15 | cm$^3$/cm$^3$ |
| soil saturation - $S_L$ | [10] | 24 | % |
| soil moisture (grav) – w | [7] | 0.15 | g/g |
| air filled porosity – a | [9] | 0.47 | cm$^3$/cm$^3$ |
| soil temperature – T | | 23 | °C |
| water solubility | [Table 3] | 118 | mg/l |
| vapor density | [Table 4] | 83 | ng/l |
| Henry's Law constant - $K_H$ | [12] | 6.98E-07 | unitless |
| soil-water partition coeff – $K_d$ | [13] | 0.9 | cm$^3$/g |
| soil sp. surface area | | 23.0 | m$^2$/g |
| soil moisture at 10 mono layers | [31] | 0.064 | g/g |
| $A_0$ | | 15.3 | |
| B(w) | [30] | 6.2 | |
| Alpha - $\alpha$ | | 51.2 | |
| A | [28] | 6.18 | |
| $K_{d'}$ (w)= $10^A$ | | 1.52E+06 | cm$^3$/g |
| Soil-Gas Partition Coeff-$K_{SG}$ | [26] | 1.47E+04 | cm$^3$/g |
| Gas Partitioning Factor-$R_G$ | [23] | 1.52E+06 | cm$^3$/cm$^3$ |
| Liquid Partitioning Factor –$R_L$ | [22] | 1.06E+00 | |
| Solid-Liquid Partitioning Factor – $R_{SL}$ | [24] | 1.18E+00 | |
| Solid-Gas Partitioning Factor – $R_{SG}$ | [25] | 1.04E+02 | |
| Total Soil Concentration - $C_T$ | | 1,000 | ng/g |
| Total Soil Concentration - $C_T$ | | 1.00E+00 | µg/cm$^3$ |
| Total Solid Phase Concentration – $C_S$ | [21] | 0.86 | µg/cm$^3$ |
| Total Liquid Phase Concentration - $C_L$ | [21] | 0.94 | mg/L |
| Total Vapor Phase Concentration - $C_G$ | [21] | 0.658 | ng/L |
| Total Vapor Phase Concentration - $C_G$ | [21] | 70.347 | ppt |
| Mass Fraction, Solid - $f_S$ | [34] | 0.86 | |
| Mass Fraction, Liquid - $f_L$ | [35] | 0.14 | |
| Mass Fraction, Gas - $f_G$ | [36] | 0.0000003 | |
| Mass Fraction, Total | [37] | 1.000000000 | |

Gray cell – input
Black cell – output

Table 13. DNT Phase Partitioning Estimation Spreadsheet

| Parameter [equation] | | Value | Units |
|---|---|---|---|
| soil bulk density - $\rho_b$ | [3] | 1 | $g/cm^3$ |
| soil particle density - $\rho_s$ | | 2.6 | $g/cm^3$ |
| soil porosity - $\varphi$ | [4] | 0.62 | $cm^3/cm^3$ |
| soil moisture (vol) - $\theta$ | [6] | 0.15 | $cm^3/cm^3$ |
| soil saturation - $S_L$ | [10] | 24 | % |
| soil moisture (grav) – w | [7] | 0.15 | g/g |
| air filled porosity – a | [9] | 0.47 | $cm^3/cm^3$ |
| soil temperature – T | | 23 | °C |
| water solubility | [Table 3] | 186 | mg/l |
| vapor density | [Table 4] | 1618 | ng/l |
| Henry's Law constant - $K_H$ | [12] | 8.72E-06 | unitless |
| soil-water partition coeff – $K_d$ | [13] | 0.5 | $cm^3/g$ |
| soil sp. surface area | | 23.0 | $m^2/g$ |
| soil moisture at 10 mono layers | [31] | 0.064 | g/g |
| $A_0$ | | 13.1 | |
| B(w) | [30] | 4.9 | |
| Alpha - $\alpha$ | | 43.5 | |
| A | [28] | 4.88 | |
| $K_d$, (w)= $10^A$ | | 7.67E+04 | $cm^3/g$ |
| Soil-Gas Partition Coeff-$K_{SG}$ | [26] | 2.10E+03 | $cm^3/g$ |
| Gas Partitioning Factor-$R_G$ | [23] | 7.67E+04 | $cm^3/cm^3$ |
| Liquid Partitioning Factor –$R_L$ | [22] | 6.68E-01 | |
| Solid-Liquid Partitioning Factor – $R_{SL}$ | [24] | 1.34E+00 | |
| Solid-Gas Partitioning Factor – $R_{SG}$ | [25] | 3.65E+01 | |
| Total Soil Concentration - $C_T$ | | 1,000 | ng/g |
| Total Soil Concentration - $C_T$ | | 1.00E+00 | $\mu g/cm^3$ |
| Total Solid Phase Concentration – $C_S$ | [21] | 0.77 | $\mu g/cm^3$ |
| Total Liquid Phase Concentration - $C_L$ | [21] | 1.51 | mg/L |
| Total Vapor Phase Concentration - $C_G$ | [21] | 13.21 | ng/L |
| Total Vapor Phase Concentration - $C_G$ | [21] | 1761.939 | ppt |
| Mass Fraction, Solid - $f_S$ | [34] | 0.78 | |
| Mass Fraction, Liquid - $f_L$ | [35] | 0.22 | |
| Mass Fraction, Gas - $f_G$ | [36] | 0.0000061 | |
| Mass Fraction, Total | [37] | 1.000000000 | |

Gray cell – input
Black cell – output

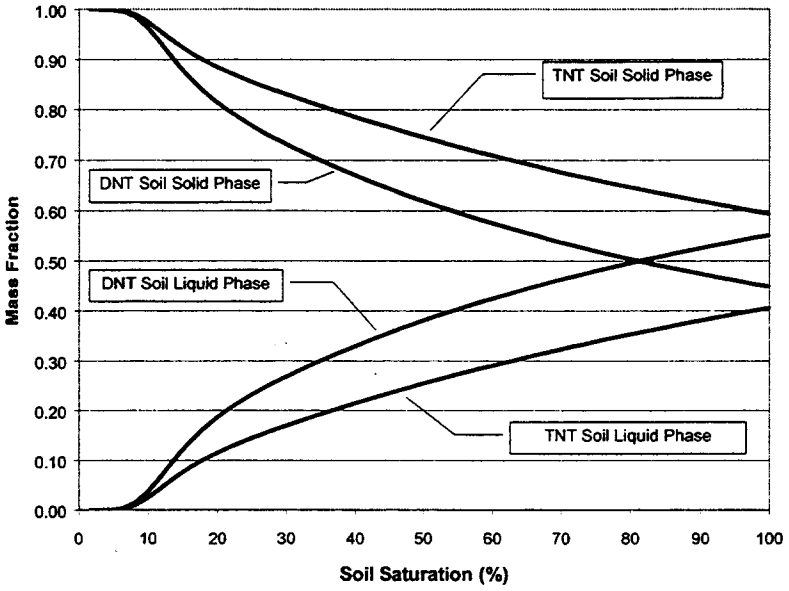


Figure 24. Soil Solid and Liquid Phase Mass Fractions

The effect of the vapor-solid partitioning process is more evident on the vapor mass fraction as shown in Figure 25. Starting at about ten percent saturation, the vapor mass fraction declines by a factor of about $10^5$. At the high-end saturation, the vapor mass fraction also declines as the air filled porosity goes to zero.

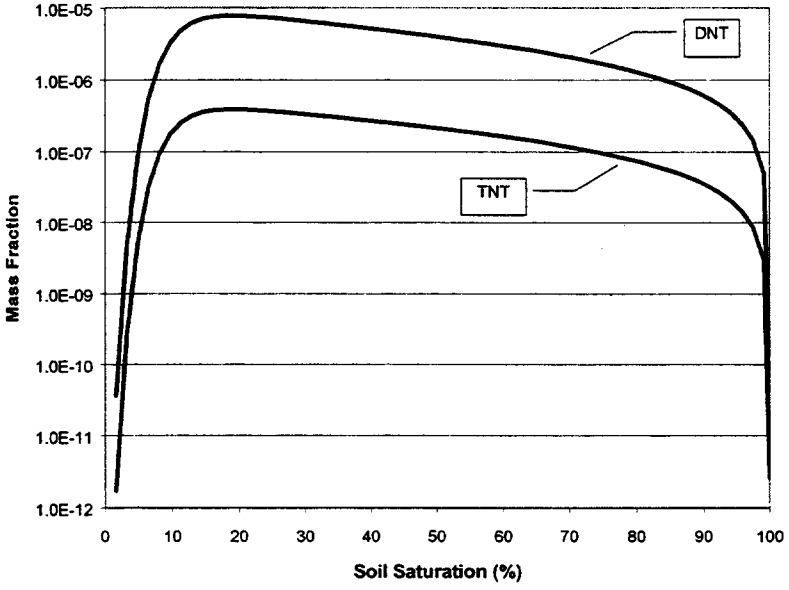


Figure 25. Soil Vapor Mass Fraction

To evaluate the effect of $K_d$ on solid and liquid phase mass fraction, $K_d$ was changed down to 0.5 and up to 3.0 ml/g as shown in Figure 26 for TNT. This range of $K_d$ is likely typical for most soils; however, one can see that solid and liquid phase mass fraction is very sensitive to $K_d$. Figure 27 shows the effect of $K_d$ on the vapor mass fraction. Since the vapor mass fraction is strongly controlled by $K_H$, which is affected by the liquid phase mass fraction, the effect of $K_d$ on

vapor phase mass fraction is approximately the same as for the liquid phase mass fraction in the range of 10 to 90 percent saturation. At the extremes, the effect of vapor-solid partitioning (low saturation) and diminished soil air porosity (high end) becomes prominent.

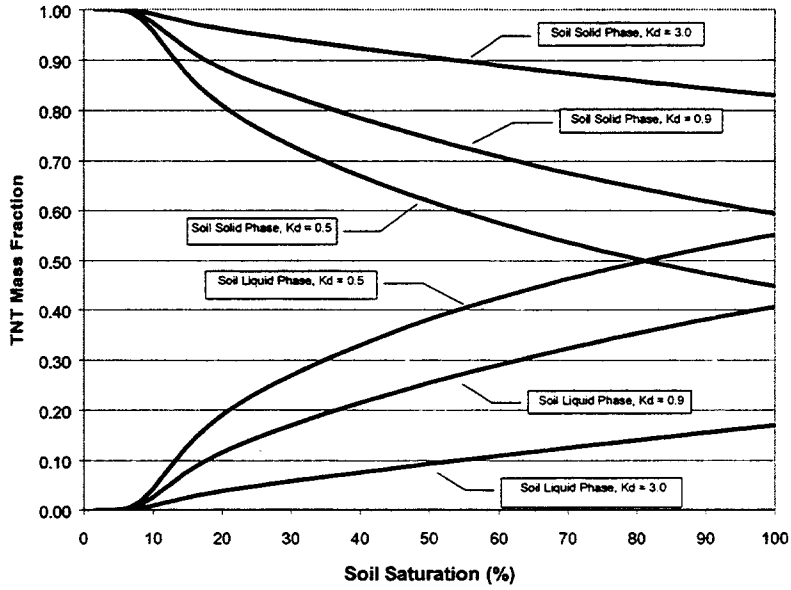


Figure 26. Effect of $K_d$ on TNT Solid and Liquid Mass Fraction

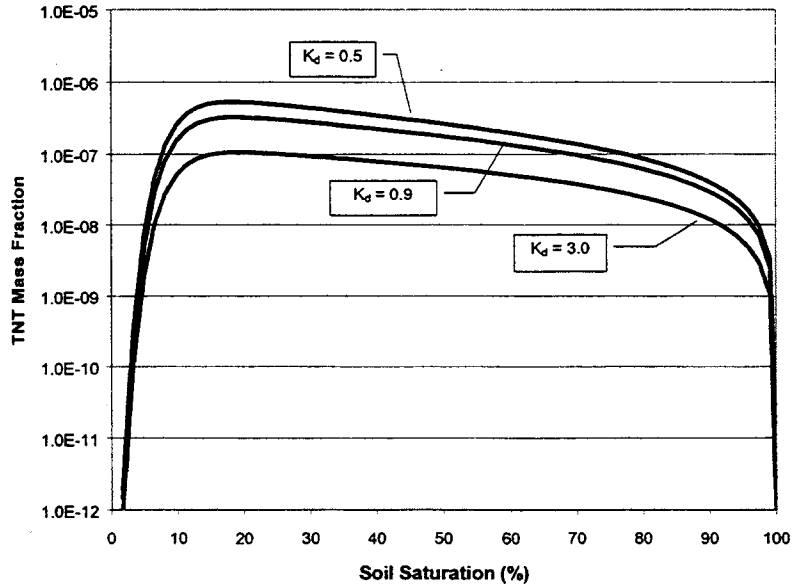


Figure 27. Effect of $K_d$ on Vapor Mass Fraction

Temperature does have an effect on $K_H$, as it affects both aqueous solubility and vapor pressure. Figure 28 shows the effect of increasing the temperature to 45°C ($K_d$ = 0.9 mL/g) and decreasing the temperature to 5°C ($K_d$ = 0.9 mL/g) for the TNT vapor mass fraction. Decreasing the temperature to 5°C has the effect of decreasing the vapor phase mass fraction by a factor of 10, while increasing the temperature to 45°C has the effect of increasing the vapor phase mass fraction by a factor of about 5.

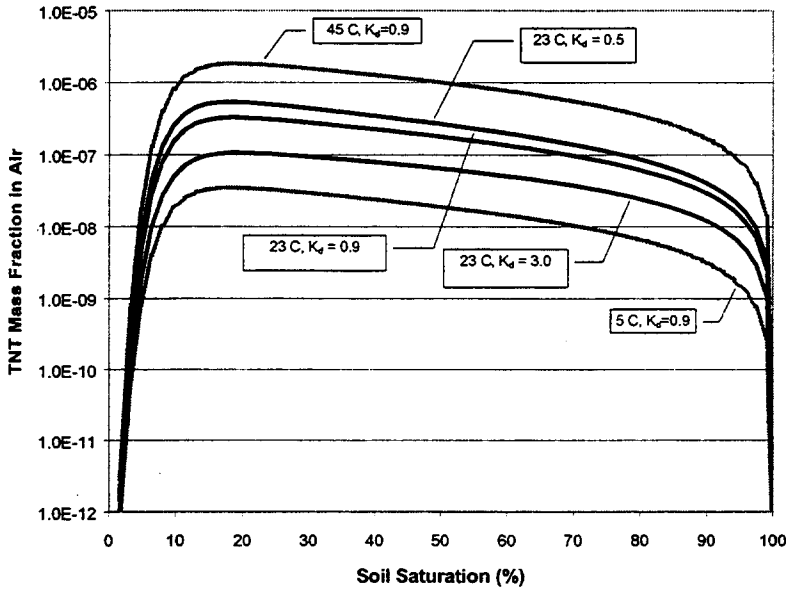


Figure 28. Effect of Temperature on TNT Vapor Mass Fraction

# 6.0 Vapor Sensing Performance Requirements

From the discussion in Section 5.0, one can see that for any value of total TNT or DNT residue in the soil ($C_T$), there can be quite a range of vapor concentrations depending on the temperature, soil-water partitioning coefficient ($K_d$), and soil saturation. This range may span a factor of about 100 for damp soils ($10\%<S_L<90\%$) and about 10,000 for dry soils ($S_L<10\%$).

Notwithstanding the uncertainties in the model input parameters and experimental methods, it appears that soil to soil gas correlation is adequate for the task of developing performance standards for vapor detection of soil residues containing DNT and TNT. With measured soil residues of DNT and TNT adjacent to UXO or landmines, an estimate of the vapor concentration can be completed using the equations shown above and with the data input embodied in Tables 12 and 13. These vapor concentrations can then be used to establish performance requirements for chemical sensing equipment.

Figure 29 shows performance requirements for chemical sensing of various total TNT soil residues ($C_T$) approximating those found near buried landmines (Jenkins et al., 2000), where most surface soil values ranged from 1 to 100 ng/g. These estimates were derived from input parameters shown in Table 12 varying the moisture content and the total soil concentration ($C_T$). Figure 30 shows performance requirements for DNT using the input parameters shown in Table 13. For the same total soil residue ($C_T$), the vapor concentrations of DNT are about a factor of 20 greater than TNT due in combination to a greater $K_H$ and lower $K_d$.

From these figures, it appears that vapor-sensing equipment must have sensitivities in the range of 1 to 10 ppt for damp soils ($w > 0.10$ g/g) and sub ppt for the varying degrees of soil moisture as the soil dries. This is, however, a hypothetical case under steady state conditions. The values shown here are for vapors in equilibrium with a single soil type in a closed space. Variations in soil type will cause changes in $K_d$ and $K_d(w)$ that are unknown at this time. For vapor sensing of surface soil, the unmixed boundary layer may be very small. Beyond this, dilution will decrease the vapor concentration enormously. Vapor sampling equipment that disturbs the surface boundary layer will also undoubtedly collect much reduced vapor concentrations. And, there is much uncertainty in the transient period in the release of vapors from dry soils upon wetting.

Nevertheless, these figures of merit for vapor sampling are needed to direct improvements in landmine detection using chemical sensing. Notwithstanding the challenges of solid to vapor or liquid phase transfer, sampling soil solid phases will collect more analyte mass given the tremendous phase partitioning favor and preconcentration effect over the vapor phase. This alternative may be valuable in certain circumstances, until vapor sampling and sensing technology can routinely measure these extremely low levels.

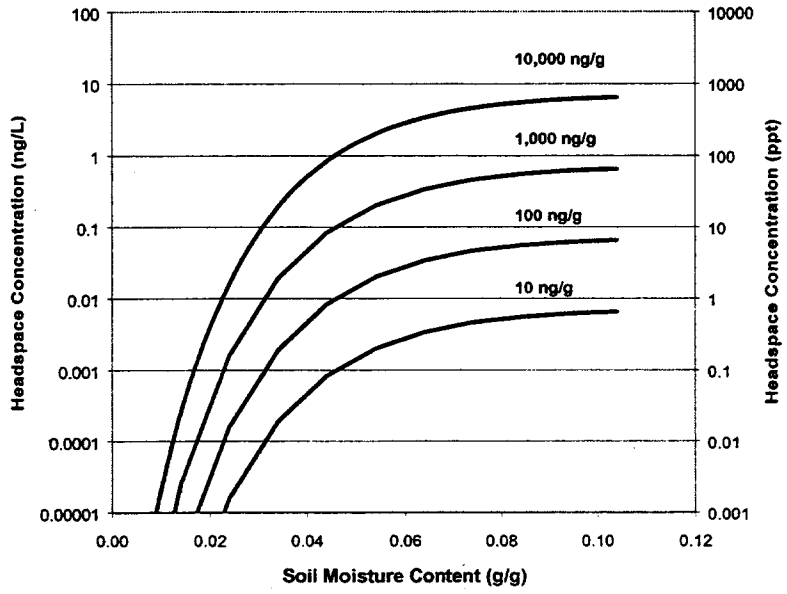


Figure 29. TNT Vapor Sensing Performance Requirements for Various Total Soil Residues

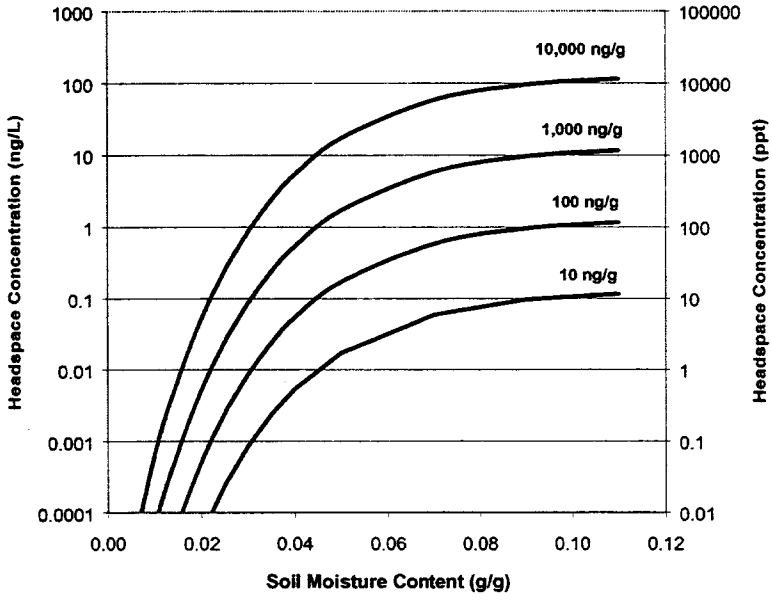


Figure 30. DNT Vapor Sensing Performance Requirements for Various Total Soil Residues

# References


1) Army Materiel Command. 1971. *Engineering Design Handbook: Explosive Series, Properties of Explosives of Military Interest.* Headquarters, U.S. Army Materiel Command, AMCP 706-177, Washington, D.C. January 1971.
2) Burglsser, C.S., M. Cernik, M. Borkovec and H. Sticher. 1993. Determination of Nonlinear Adsorption Isotherms from Column Experiments: An Alternative to Batch Studies. Environ. Sci. Technol., Vol. 27, No. 5, 943-948.
3) Farmer, W.J., M.S. Yang, J. Letey, and W.F. Spencer. 1980. Hexachlorobenzene: its vapor pressure and vapor phase diffusion in soil. Soil Sci. Soc. Am. Proc. 44:676-680.
4) George, V., Jenkins, T.F.; Phelan, J.M.; Leggett, D.C.; Oxley, J.;Webb, S.W.;Miyares, P.;Cragin, J.;Smith, J.;and T.E. Berry. 2000. Progress on Determining the Vapor Signature of a Buried Landmine. Proceedings of the SPIE 14th Annual International Symposium on Aerospace/Defense Sensing, Simulation and Controls, Detection and Remediation Technologies for Mines and Minelike Targets V, April 24-28, 2000, Orlando, FL.
5) Jenkins, T.F., D.C. Leggett, and T.A. Ranney. 1999. Vapor Signatures from Military Explosives. Part 1. Vapor Transport from Buried Military-Grade TNT. U.S. Army Corps of Engineers, Engineer Research and Development Center, Special Report 99-21, Hanover, New Hampshire, December 1999.
6) Jenkins, T.F., M.E. Walsh, P.H. Miyares, J. Kopczynski, T. Ranney, V. George, J.C. Pennington, and T.E. Berry, Jr.. 2000. Analysis of Explosives-Related Chemical Signatures in Soil Samples Collected Near Buried Land Mines. U.S. Army Corps of Engineers, Engineer Research and Development Center, ERDC TR-00-5, Hanover, New Hampshire, August 2000.
7) Jury, W.A., R. Grover, W.F. Spencer, and W. J. Farmer. 1980. Modeling Vapor Lossess of Soil-Incorporated with Triallate. Soil Sci. Soc. of Am. J., 44, 445-50 (May-June 1980).
8) Jury, W.A., W.F. Spencer, and W.J. Farmer. 1983. Behavior Assessment Model for Trace Organics in Soil: I. Model Description. J. Environ. Qual., Vol 12, no. 4, 558-564.
9) Jury, W.A., W.J. Farmer, and W.F. Spencer. 1984a. Behavior Assessment Model for Trace Organics in Soil: II. Chemical Classification and Parameter Sensitivity. J. Environ. Qual., Vol. 13, no. 4, 567-572.
10) Jury, W.A., W.F. Spencer, and W.J. Farmer. 1984b. Behavior Assessment Model for Trace Organics in Soil: III. Application of Screening Model. J. Environ. Qual., Vol 13, no. 4, 573-579.
11) Jury, W.A., W.F. Spencer, and W.J. Farmer. 1984c. Behavior Assessment Model for Trace Organics in Soil: IV. Review of Experimental Evidence. J. Environ. Qual., Vol 13, no. 4, 580-586.
12) Jury, W.A., D. Russo, G. Streile, and H. Abd. 1990. Evaluation of Volatilization by Organic Chemicals Residing Below the Surface. Water Resources Research, Vol 26, no 1, p 13-20, January 1990.
13) Jury, W.A., W.R. Gardner and W.H. Gardner. 1991. Soil Physics, Fifth Edition. John Wiley and Sons, Inc.
14) Kaye, S.M. 1980. Encyclopedia of Explosives and Related Items. Volume 9. U.S. Army Armament Research and Development Command, Large Caliber Weapon Systems Laboratory, Dover, NJ. 1980.
15) Mayer, R., J. Letey, and W.J. Farmer. 1974. Models for predicting volatilization of soil-incorporated pesticides. Soil Sci. Soc. Am. Proc. 38:563-568.
16) McGrath, C.J. 1995. Review of formulations for Processes Affecting the Subsurface Transport of Explosives. Technical Report IRRP-95-2; U.S. Army Engineer Waterways Experiment Station: Vicksburg, MS, 1995.
17) Ong, S.K. and L.W. Lion. 1991a. Mechanisms for trichloroethylene vapor sorption onto soil minerals. J. Environ Qual. 20:180-188.
18) Ong, S.K. and L.W. Lion. 1991b. Effects of soil properties and moisture on the sorption of trichloroethylene vapor. Water Res. 25:29-36.
19) Ong, S.K., T.B. Culver, L.W. Lion, and C.A. Shoemaker. 1992. Effects of soil moisture and physical-chemical properties of organic pollutants on vapor-phase transport in the vadose zone. Journal of Contaminant Hydrology, 11(1992) 273-290.
20) Pella, P.A. 1977. Measurement of the vapor pressures of TNT, 2,4-DNT, 2,6-DNT and EGDN. J. chem. thermodynamics, 1977, 9, 301-305.

21) Pennington, J.C. and W.H. Patrick. 1990. Adsorption and Desportion of 2,4,6-Trinitrotoluene by Soils. J. Environ. Qual. 19:559-567 (1990).
22) Pennington, J.C., C.A. Hayes, S.L. Yost, P.Miyares, T.Jenkins. 1999. Partioning Coefficients on Fort Leonard Wood Soils. Draft Report, U.S. Army Corps of Engineers, Waterways Experiment Station, September 1, 1999.
23) Petersen, L.W., P. Moldrup, Y.H.El-Farhan, O.H. Jacobsen, T. Yamaguchi, and D.E. Rolston. 1995. The Effect of Moisture and Soil Texture on the Adsorption of Organic Vapors. J. Environ. Qual. 24:752-759. (1995).
24) Petersen, L.W., Y.H. El-Farhan, P. Moldrup, D.E. Rolston and T. Yamaguchi. 1996. Transient Diffusion, Adsorption and Emission of Volatile Organic Vapors in Soils with Fluctuating Low Water Contents. J. Environ. Qual. 25:1054-1063 (1996).
25) Peterson, M.S., L.W. Lion,and C.A. Shoemaker. 1988. Influence of Vapor-Phase Sorption and Diffuson on the Fate of Trichloroethylene in an Unsaturated Aquifer System. Environ. Sci. Technol. 1988, 22, 571-578.
26) Phelan, J.M. and J.L. Barnett. 2001. Solubility of 2,4-Dinitrotoluene and 2,4,6-Trinitrotoluene in Water. J. Chem. Eng. Data, accepted for publication, Apr/May 2001.
27) Phelan, J.M., Gozdor, M., Webb, S.W., and M. Cal. 2000. "Laboratory Data and Model Comparisons of the Transport of Chemical Signatures From Buried Landmines/UXO" in *Proceedings of the SPIE 14th Annual International Symposium on Aerospace/Defense Sensing, Simulation and Controls, Detection and Remediation Technologies for Mines and Minelike Targets V,* April 24-28, 2000, A.C. Dubey, J.F. Harvey, J.T. Broach, R.E. Dugan, eds.
28) Phelan, J.M. and S.W. Webb. 1998a, "Chemical Detection of Buried Landmines," Proceedings of the 3rd International Symposium on Technology and the Mine Problem, April 6-9, 1998. Mine Warfare Association.
29) Phelan, J.M. and S.W. Webb. 1998b, "Simulation of the Environmental Fate and Transport of Chemical Signatures from Buried Landmines," International Symposium on Aerospace/Defense Sensing, Simulation, and Controls, Orlando, FL, April 13-17, 1998, SPIE.
30) Phelan, J.M.; Webb, S.W., 1997. Environmental Fate and Transport of Chemical Signatures from Buried Landmines - Screening Model Formulation and Initial Simulations. Sandia National Laboratories Report SAND97-1426, Albuquerque, NM. June 1997.
31) Ro, Kyoung S.; Venugopal, Asha; Adrian, D. Dean; Constant, D.; Qaisi, Kamel; Valsaraj, Kalliat T.; Thibodeaux, Louis J.; and, Roy, Dipak. 1996. Solubility of 2,4,6-Trinitrotoluene in Water. J. Chem. Eng. Data 1996, 41, 758-761.
32) Rosenblatt, D.H.; Burrows, E.P.; Mitchell, W.R.; and, D.L. Parmer. 1991. Organic Explosives and Related Compounds. In *The Handbook of Environmental Chemistry*; Hutzinger, O. Ed.; Springer-Verlag: New York, 1991; Volume 3, Part G.
33) Spanggord, R.J.; Mabey, W.R.; Mill, T.; Chou, T.W.; Smith, J.H.; Less, S.; and D. Robert. 1983. Environmental Fate Studies on Certain Munitions Wastewater Constituents. LSU-7934, AD-A138550; SRI International: Menlo Park, CA, 1983.
34) Stephen, H. and T. Stephen. 1963. *Solubilities of Inorganic and Organic Compounds;* MacMillian Co.; New York, 1963; Vol.1 Part 1.
35) Taylor, C.A. and W. H. Rinkenbach. 1923. The Solubility of Trinitrotoluene in Organic Solvents. Ind. Eng. Chem., 15, 795 (1923).
36) Urbanski, T. 1964. *Chemistry and Technology of Explosives*; MacMillian Co.; New York, 1964; vol I.
37) Verschueren, K.. 1983. *Handbook of Environmental Data on Organic Chemicals*, 2nd ed.; Van Nostrand Reinhold Co.; New York, 1983.
38) Webb, S.W., K. Pruess, J. M. Phelan and S.A. Finsterle. 1999. Development of a Mechanistic Model for the Movement of Chemical Signatures from Buried Landmines/UXO. Proceedings of SPIE Conference on Detection and Remediation Technologies for Mines and Minelike Targets IV. April 5-9, 1999. Orlando, FL.

## Distribution:

| | | |
|---|---|---|
| 1 | MS0719 | W.B.Cox, 6131 |
| 20 | MS0719 | J.M. Phelan, 6131 |
| 1 | MS0719 | S.W. Webb, 6131 |
| 1 | MS1452 | J.A. Merson, 2552 |
| 1 | MS1452 | P.J. Rodacy, 2552 |
| 1 | MS1452 | J.L. Barnett, 2552 |
| 1 | MS0860 | R.J. Simonson, 2618 |
| 1 | MS9018 | Central Technical Files, 8945-1 |
| 2 | MS0899 | Technical Library, 9616 |
| 1 | MS0612 | Review and Approval Desk, 9612 for DOE/OSTI |

Ms. Vivian George
Draper Laboratories
PM-MCD
AMSTA-LC-AD
10205 Burbeck Rd
Fort Belvoir, VA 22060-5811

Dr. Tom Jenkins
U.S. Army Corps of Engineers
72 Lyme Road
Hanover, NH 03755

Ms. Lena Sarholm
Swedish Defence Research Agency, FOI
Division of Energetic Materials
Grindsjön
SE-147 25 Tumba
Sweden

Dr. Bjarne Haugstad
Forsvarets Forskningsinstitutt
Norweigian Defence Research Establishment
Division for Weapons and Material
P.O. Box 25, NO-2027
Kjeller, Norway

Mr. Havard Bach
Geneva International Center for Humanitarian Demining
Av. de la Paix 7bis
Post Box 1300
1211 Geneva 1
Switzerland

Dr. Jeff Marqusee
Strategic Environmental Research and Development Program
901 North Stuart Street, Suite 303
Arlington, VA 22203